Numerische Mathematik (2021) 147:127–155
https://doi.org/10.1007/s00211-020-01166-4

Numerische Mathematik

Development and analysis of a new finite element method for the Cohen–Monk PML model

Meng Chen[1] · Yunqing Huang[2] · Jichun Li[3]

Received: 10 April 2019 / Revised: 17 November 2020 / Accepted: 17 November 2020 /
Published online: 2 January 2021

Abstract
This work deals with the Cohen–Monk Perfectly Matched Layer (PML) model. We first carry out the stability analysis of its equivalent form. Then we propose and analyse a finite element scheme for solving this equivalent PML model. Discrete stability and optimal error estimate are established. Numerical results are presented to justify the analysis and effectiveness of this PML model. This paper presents the first mathematical analysis for this PML model and the corresponding numerical analysis for the proposed finite element scheme.

Mathematics Subject Classification 65N30 · 35L15 · 78-08

1 Introduction

Since the introduction of the Perfectly Matched Layer (PML) by Bérenger in 1994 [4] for solving the time-dependent Maxwell's equations in unbounded domains, it has become almost the exclusive choice for wave propagation simulation. Since 1994,

Partially supported by NSF of China Project No. 11971410, and NSF Grant DMS-20-11943, NNSFC (No. 11961036).

✉ Jichun Li
jichun.li@unlv.edu

Meng Chen
pp756230872@126.com

Yunqing Huang
huangyq@xtu.edu.cn

1 School of Mathematics and Statistics, Jiangxi Normal University, Nanchang 330022, Jiangxi, China

2 Hunan Key Laboratory for Computation and Simulation in Science and Engineering, Xiangtan University, Xiangtan, China

3 Department of Mathematical Sciences, University of Nevada Las Vegas, Las Vegas, NV 89154-4020, USA

many PML models have been proposed and studied, and its applications have been extended to acoustic wave, elastodynamics wave, and electromagnetic wave propagation in complex media [1,3]. Due to the complexity of PML governing equations, compared to many engineering papers on PML models and their applications (see [17, Ch.7], [14, Ch.8] and references therein), publications on the mathematical analysis of PML and numerical analysis of various numerical methods developed for solving the time-domain PML models are quite limited [2,5,6,8,11,13,15].

Back in 1999, by using the stretched coordinates approach, Cohen and Monk [7] developed a PML model and proposed using mapped mass-lumped edge elements to solve it. In 2014, we [9] carried out the well-posedness study of this Cohen–Monk PML model by proving the existence and uniqueness, and stability of this PML model. However, we were unable to establish the numerical stablity for both the original finite element scheme proposed by Cohen and Monk [7] and a new scheme proposed by us in [9]. This paper is our continuous effort on studying this PML model. More specifically, by reformulating the Cohen–Monk PML model into another equivalent form, we manage to prove its stability, which is different from that obtained in [9]. Then we propose a finite element scheme for this equivalent PML model. By following the proof technique developed for the continuous stability analysis, we establish a discrete stability which has exactly the same form as the continuous stability. To the best of our knowledge, this is the first paper which establishes a complete numerical stability and error estimate for a finite element scheme developed to solve this PML model.

The rest of the paper is organized as follows. In Sect. 2, we first establish the equivalent Cohen–Monk PML model, and then prove its stability. In Sect. 3, we propose a fully-discrete finite element scheme for this equivalent PML model, and prove both the discrete stability and optimal error estimate of the scheme. Numerical results are presented in Sect. 4 to demonstrate the correct implementation of our scheme and the performance of this equivalent PML model. We conclude the paper in Sect. 5.

2 The Cohen–Monk PML model and its analysis

The governing equations of the Cohen–Monk PML model are given as follows [7]:

$$\epsilon_0 \frac{\partial \boldsymbol{E}^*}{\partial t} - \nabla \times \boldsymbol{H} = 0, \tag{1}$$

$$\mu_0 \frac{\partial \boldsymbol{H}^*}{\partial t} + \nabla \times \boldsymbol{E} = 0, \tag{2}$$

$$\frac{\partial^2 \boldsymbol{E}}{\partial t^2} + C_m \frac{\partial \boldsymbol{E}}{\partial t} + D\boldsymbol{E} = \frac{\partial^2 \boldsymbol{E}^*}{\partial t^2} + G \frac{\partial \boldsymbol{E}^*}{\partial t}, \tag{3}$$

$$\frac{\partial^2 \boldsymbol{H}}{\partial t^2} + C_m \frac{\partial \boldsymbol{H}}{\partial t} + D\boldsymbol{H} = \frac{\partial^2 \boldsymbol{H}^*}{\partial t^2} + G \frac{\partial \boldsymbol{H}^*}{\partial t}, \tag{4}$$

where ϵ_0 and μ_0 are the vacuum permittivity and permeability, respectively, $\boldsymbol{E}(\mathbf{x}, t)$ and $\boldsymbol{H}(\mathbf{x}, t)$ are the electric and magnetic fields, respectively, and $\boldsymbol{E}^*(\mathbf{x}, t)$ and $\boldsymbol{H}^*(\mathbf{x}, t)$ are the auxiliary electric and magnetic fields, respectively. Moreover, the 3×3 diagonal matrices C_m, D and G are given by

$$C_m = diag(\sigma_2 + \sigma_3, \sigma_1 + \sigma_3, \sigma_1 + \sigma_2), D = diag(\sigma_2\sigma_3, \sigma_1\sigma_3, \sigma_1\sigma_2),$$
$$G = diag(\sigma_1, \sigma_2, \sigma_3), \tag{5}$$

where σ_1, σ_2 and σ_3 are nonnegative functions and represent the damping variations along the x, y, and z directions, respectively.

To investigate the well-posedness of the model problem (1)–(4), we assume that (1)–(4) hold in the domain [7]

$$\Omega = (R^3 \setminus \overline{S}) \cap ([-L_1 - \delta_1, L_1 + \delta_1] \times [-L_2 - \delta_2, L_2 + \delta_2] \times [-L_3 - \delta_3, L_3 + \delta_3]),$$

where S denotes the perfectly conducting (PEC) scatter, $\delta_i > 0, i = 1, 2, 3$, is the thickness of the PML in the x, y, and z directions, respectively. Furthermore, the entire scatter is assumed to be contained in the hexahedron $[-L_1, L_1] \times [-L_2, L_2] \times [-L_3, L_3]$, and the problem (1)–(4) satisfies the PEC boundary condition

$$\boldsymbol{n} \times \boldsymbol{E} = 0 \quad on \;\; \partial\Omega = \Gamma_s \cup \Gamma_\infty, \tag{6}$$

where $\boldsymbol{n}$ is the unit outward normal to the scatter boundary Γ_s and the boundary Γ_∞ of the box $[-L_1 - \delta_1, L_1 + \delta_1] \times [-L_2 - \delta_2, L_2 + \delta_2] \times [-L_3 - \delta_3, L_3 + \delta_3]$. Finally, we assume that (1)–(4) is supplemented with the initial conditions

$$\begin{aligned} \boldsymbol{E}(\mathbf{x}, 0) = \boldsymbol{E}_0(\mathbf{x}), \;\; \boldsymbol{H}(\mathbf{x}, 0) = \boldsymbol{H}_0(\mathbf{x}), \\ \boldsymbol{E}^*(\mathbf{x}, 0) = \boldsymbol{E}_0^*(\mathbf{x}), \;\; \boldsymbol{H}^*(\mathbf{x}, 0) = \boldsymbol{H}_0^*(\mathbf{x}), \end{aligned} \tag{7}$$

where $\boldsymbol{E}_0(\mathbf{x})$, $\boldsymbol{H}_0(\mathbf{x})$, $\boldsymbol{E}_0^*(\mathbf{x})$ and $\boldsymbol{H}_0^*(\mathbf{x})$ are some given functions.

We integrate the model Eqs. (3) and (4) with respect to time once and obtain the following PML equations:

$$\epsilon_0 \frac{\partial \boldsymbol{E}^*}{\partial t} - \nabla \times \boldsymbol{H} = 0, \tag{8}$$

$$\mu_0 \frac{\partial \boldsymbol{H}^*}{\partial t} + \nabla \times \boldsymbol{E} = 0, \tag{9}$$

$$\frac{\partial \boldsymbol{E}}{\partial t} + C_m \boldsymbol{E} + D \int_0^t \boldsymbol{E} dt = \frac{\partial \boldsymbol{E}^*}{\partial t} + G\boldsymbol{E}^* + \boldsymbol{f}, \tag{10}$$

$$\frac{\partial \boldsymbol{H}}{\partial t} + C_m \boldsymbol{H} + D \int_0^t \boldsymbol{H} dt = \frac{\partial \boldsymbol{H}^*}{\partial t} + G\boldsymbol{H}^* + \boldsymbol{g}, \tag{11}$$

where $\boldsymbol{f} = \frac{\partial \boldsymbol{E}}{\partial t}(\mathbf{x}, 0) + C_m \boldsymbol{E}(\mathbf{x}, 0) - \frac{\partial \boldsymbol{E}^*}{\partial t}(\mathbf{x}, 0) - G\boldsymbol{E}^*(\mathbf{x}, 0)$ and $\boldsymbol{g} = \frac{\partial \boldsymbol{H}}{\partial t}(\mathbf{x}, 0) + C_m \boldsymbol{H}(\mathbf{x}, 0) - \frac{\partial \boldsymbol{H}^*}{\partial t}(\mathbf{x}, 0) - G\boldsymbol{H}^*(\mathbf{x}, 0)$ are time-independent function.

Denote $\boldsymbol{J}(\boldsymbol{x}, t) = \int_0^t \boldsymbol{E} dt$ and $\boldsymbol{K}(\boldsymbol{x}, t) = \int_0^t \boldsymbol{H} dt$, which imply that $\boldsymbol{J}(\boldsymbol{x}, 0) := \boldsymbol{J}_0(\boldsymbol{x}) = 0$ and $\boldsymbol{K}(\boldsymbol{x}, 0) := \boldsymbol{K}_0(\boldsymbol{x}) = 0$. Hence, we obtain the following new equivalent governing equations for the Cohen–Monk PML model:

$$\frac{\partial \boldsymbol{J}}{\partial t} = \boldsymbol{E}, \tag{12}$$

$$\frac{\partial \boldsymbol{K}}{\partial t} = \boldsymbol{H}, \tag{13}$$

$$\epsilon_0 \frac{\partial \boldsymbol{E}^*}{\partial t} - \nabla \times \boldsymbol{H} = 0, \tag{14}$$

$$\mu_0 \frac{\partial \boldsymbol{H}^*}{\partial t} + \nabla \times \boldsymbol{E} = 0, \tag{15}$$

$$\frac{\partial \boldsymbol{E}}{\partial t} + C_m \boldsymbol{E} + D\boldsymbol{J} = \frac{\partial \boldsymbol{E}^*}{\partial t} + G\boldsymbol{E}^* + \boldsymbol{f}, \tag{16}$$

$$\frac{\partial \boldsymbol{H}}{\partial t} + C_m \boldsymbol{H} + D\boldsymbol{K} = \frac{\partial \boldsymbol{H}^*}{\partial t} + G\boldsymbol{H}^* + \boldsymbol{g}, \tag{17}$$

subject to the initial conditions

$$\begin{aligned} \boldsymbol{E}(\mathbf{x},0) = \boldsymbol{E}_0(\mathbf{x}), \boldsymbol{H}(\mathbf{x},0) = \boldsymbol{H}_0(\mathbf{x}), \boldsymbol{E}^*(\mathbf{x},0) = \boldsymbol{E}_0^*(\mathbf{x}), \boldsymbol{H}^*(\mathbf{x},0) \\ = \boldsymbol{H}_0^*(\mathbf{x}), \boldsymbol{J}(\mathbf{x},0) = \boldsymbol{K}(\mathbf{x},0) = 0, \end{aligned} \tag{18}$$

where $\boldsymbol{E}_0(\mathbf{x}), \boldsymbol{H}_0(\mathbf{x}), \boldsymbol{E}_0^*(\mathbf{x}), \boldsymbol{H}_0^*(\mathbf{x})$ are some given functions.

Some common notation are used in the rest paper [14,16]:

$$H(div,\Omega) = \left\{ \boldsymbol{u} \in (L^2(\Omega))^3; \nabla \cdot \boldsymbol{u} \in L^2(\Omega) \right\},$$

$$H(curl;\Omega) = \{ \boldsymbol{u} \in (L^2(\Omega))^3 : \nabla \times \boldsymbol{u} \in (L^2(\Omega))^3 \},$$

$$H_0(curl;\Omega) = \{ \boldsymbol{u} \in H(curl;\Omega) : \mathbf{n} \times \boldsymbol{u} = 0, \ \ on \ \partial\Omega \},$$

with equipped norms

$$\|\boldsymbol{u}\|_{H(div;\Omega)} = (\|\boldsymbol{u}\|_0^2 + \|\nabla \cdot \boldsymbol{u}\|_0^2)^{\frac{1}{2}}, \quad \|\boldsymbol{u}\|_{H(curl;\Omega)} = (\|\boldsymbol{u}\|_0^2 + \|\nabla \times \boldsymbol{u}\|_0^2)^{\frac{1}{2}},$$

where $\|\cdot\|_0$ denotes the standard L_2 norm in Ω. Moreover, we denote $C_v = \frac{1}{\sqrt{\epsilon_0 \mu_0}} \approx 3 * 10^8 m/s$ for the wave propagation speed in the free space.

In the rest of this section, we prove the following stability for the PML model problem (12)–(17).

Theorem 1 *For the solution* $(\boldsymbol{E}, \boldsymbol{H}, \boldsymbol{E}^*, \boldsymbol{H}^*, \boldsymbol{K}, \boldsymbol{J})$ *of* (12)–(17)*, we denote the energy*

$$\mathcal{E}(t) = \left[\frac{\epsilon_0}{2} \left(\|\boldsymbol{E}\|_0^2 + ||D^{1/2}\boldsymbol{J}||_0^2 + \|\mu_0 \boldsymbol{H}^*\|_0^2 \right) + \frac{\mu_0}{2} \left(\|\boldsymbol{H}\|_0^2 + ||D^{1/2}\boldsymbol{K}||_0^2 + \|\epsilon_0 \boldsymbol{E}^*\|_0^2 \right) \right](t), \tag{19}$$

where $D^{1/2} := diag((\sigma_2\sigma_3)^{1/2}, (\sigma_1\sigma_3)^{1/2}, (\sigma_1\sigma_2)^{1/2})$*. Then for any* $t \in (0, T]$*, we have*

$$\mathcal{E}(t) \le \frac{C_v}{C_v - 1} \cdot \exp\left(\frac{C_v}{C_v - 1} \cdot C_{stab} t\right) \left[\mathcal{E}(0) + \frac{C_v + 1}{C_v - 1} \int_0^t \left(\frac{\epsilon_0}{2} \|\boldsymbol{f}\|_0^2 + \frac{\mu_0}{2} \|\boldsymbol{g}\|_0^2\right) ds \right], \tag{20}$$

where the constant $C_{stab} := |\frac{C_m}{C_v} + C_v G|_{L^\infty(\overline{\Omega})} + 1 + \frac{|D|_{L^\infty(\overline{\Omega})}}{C_v}$.

Proof To make our proof easy to follow, we divide it into three major parts.

(I) Multiplying (16) by $\epsilon_0 \boldsymbol{E}$, multiplying (17) by $\mu_0 \boldsymbol{H}$, and integrating respective result over domain Ω, we obtain

$$\frac{\epsilon_0}{2}\frac{d}{dt}\|\boldsymbol{E}\|_0^2 + \epsilon_0(C_m\boldsymbol{E},\boldsymbol{E}) + \epsilon_0(D\boldsymbol{J},\boldsymbol{E}) = \epsilon_0(\boldsymbol{E}_t^*,\boldsymbol{E}) + \epsilon_0(G\boldsymbol{E}^*,\boldsymbol{E}) + \epsilon_0(\boldsymbol{f},\boldsymbol{E}). \tag{21}$$

and

$$\frac{\mu_0}{2}\frac{d}{dt}\|\boldsymbol{H}\|_0^2 + \mu_0(C_m\boldsymbol{H},\boldsymbol{H}) + \mu_0(D\boldsymbol{K},\boldsymbol{H}) = \mu_0(\boldsymbol{H}_t^*,\boldsymbol{H}) + \mu_0(G\boldsymbol{H}^*,\boldsymbol{H}) + \mu_0(\boldsymbol{g},\boldsymbol{H}). \tag{22}$$

Using (12) and (13), we have

$$\epsilon_0(D\boldsymbol{J},\boldsymbol{E}) = \epsilon_0(D\boldsymbol{J},\boldsymbol{J}_t) \quad \text{and} \quad \mu_0(D\boldsymbol{K},\boldsymbol{H}) = \mu_0(D\boldsymbol{K},\boldsymbol{K}_t). \tag{23}$$

Multiplying (14) by $\boldsymbol{E}$, integrating by part over domain Ω , and using PEC boundary condition (6), we obtain

$$\epsilon_0(\boldsymbol{E}_t^*,\boldsymbol{E}) = (\nabla\times\boldsymbol{H},\boldsymbol{E}) = (\nabla\times\boldsymbol{E},\boldsymbol{H}). \tag{24}$$

Multiplying (15) by $\boldsymbol{H}$, then integrating over domain Ω , we obtain

$$\mu_0(\boldsymbol{H}_t^*,\boldsymbol{H}) = -(\nabla\times\boldsymbol{E},\boldsymbol{H}). \tag{25}$$

Adding (21) and (22) together, and using (23)–(25), we obtain

$$\begin{aligned} &\frac{d}{dt}\left[\frac{\epsilon_0}{2}\left(\|\boldsymbol{E}\|_0^2 + (D\boldsymbol{J},\boldsymbol{J})\right) + \frac{\mu_0}{2}\left(\|\boldsymbol{H}\|_0^2 + (D\boldsymbol{K},\boldsymbol{K})\right)\right] \\ &\quad + \epsilon_0(C_m\boldsymbol{E},\boldsymbol{E}) + \mu_0(C_m\boldsymbol{H},\boldsymbol{H}) \\ &= \epsilon_0(G\boldsymbol{E}^*,\boldsymbol{E}) + \epsilon_0(\boldsymbol{f},\boldsymbol{E}) + \mu_0(G\boldsymbol{H}^*,\boldsymbol{H}) + \mu_0(\boldsymbol{g},\boldsymbol{H}). \end{aligned} \tag{26}$$

Integrating (26) with respect to t from 0 to t, and dropping the non-negative terms $\epsilon_0(C_m\boldsymbol{E},\boldsymbol{E})$ and $\mu_0(C_m\boldsymbol{H},\boldsymbol{H})$, we have

$$\begin{aligned} &\frac{\epsilon_0}{2}\left(\|\boldsymbol{E}\|_0^2(t) + (D\boldsymbol{J},\boldsymbol{J})(t)\right) + \frac{\mu_0}{2}\left(\|\boldsymbol{H}\|_0^2(t) + (D\boldsymbol{K},\boldsymbol{K})(t)\right) \\ &\quad \le \frac{\epsilon_0}{2}\left(\|\boldsymbol{E}\|_0^2(0) + (D\boldsymbol{J},\boldsymbol{J})(0)\right) + \frac{\mu_0}{2}\left(\|\boldsymbol{H}\|_0^2(0) + (D\boldsymbol{K},\boldsymbol{K})(0)\right) \\ &\quad + \int_0^t \left[(G\boldsymbol{E},\epsilon_0\boldsymbol{E}^*) + \epsilon_0(\boldsymbol{f},\boldsymbol{E}) + (G\boldsymbol{H},\mu_0\boldsymbol{H}^*) + \mu_0(\boldsymbol{g},\boldsymbol{H})\right] dt. \end{aligned} \tag{27}$$

(II) To control the terms $\boldsymbol{E}^*$ and $\boldsymbol{H}^*$ in (27), we multiply (16) by $\epsilon_0^2\mu_0\boldsymbol{E}^*$ and (17) by $\epsilon_0\mu_0^2\boldsymbol{H}^*$, and integrating the respective result over domain Ω, we obtain

$$\frac{\mu_0}{2}\frac{d}{dt}\|\epsilon_0\boldsymbol{E}^*\|_0^2 + \epsilon_0^2\mu_0(G\boldsymbol{E}^*, \boldsymbol{E}^*) \\ = \epsilon_0\mu_0\left[(\boldsymbol{E}_t, \epsilon_0\boldsymbol{E}^*) + (C_m\boldsymbol{E} + D\boldsymbol{J} - \boldsymbol{f}, \epsilon_0\boldsymbol{E}^*)\right], \tag{28}$$

and

$$\frac{\epsilon_0}{2}\frac{d}{dt}\|\mu_0\boldsymbol{H}^*\|_0^2 + \epsilon_0\mu_0^2(G\boldsymbol{H}^*, \boldsymbol{H}^*) \\ = \epsilon_0\mu_0\left[(\boldsymbol{H}_t, \mu_0\boldsymbol{H}^*) + (C_m\boldsymbol{H} + D\boldsymbol{K} - \boldsymbol{g}, \mu_0\boldsymbol{H}^*)\right]. \tag{29}$$

Using property $\frac{d}{dt}(u, v) = (u_t, v) + (u, v_t)$, (24) and (25), we have

$$\epsilon_0\mu_0(\boldsymbol{E}_t, \epsilon_0\boldsymbol{E}^*) = \epsilon_0\mu_0\left[\frac{d}{dt}(\boldsymbol{E}, \epsilon_0\boldsymbol{E}^*) - (\boldsymbol{E}, \epsilon_0\boldsymbol{E}_t^*)\right] \\ = \epsilon_0\mu_0\frac{d}{dt}(\boldsymbol{E}, \epsilon_0\boldsymbol{E}^*) - \epsilon_0\mu_0(\nabla\times\boldsymbol{E}, \boldsymbol{H}), \tag{30}$$

and

$$\epsilon_0\mu_0(\boldsymbol{H}_t, \mu_0\boldsymbol{H}^*) = \epsilon_0\mu_0\left[\frac{d}{dt}(\boldsymbol{H}, \mu_0\boldsymbol{H}^*) - (\boldsymbol{H}, \mu_0\boldsymbol{H}_t^*)\right] \\ = \epsilon_0\mu_0\frac{d}{dt}(\boldsymbol{H}, \mu_0\boldsymbol{H}^*) + \epsilon_0\mu_0(\nabla\times\boldsymbol{E}, \boldsymbol{H}). \tag{31}$$

Adding (28) and (29) together, and substituting (30) and (31) into the result, we obtain

$$\frac{\mu_0}{2}\frac{d}{dt}\|\epsilon_0\boldsymbol{E}^*\|_0^2 + \frac{\epsilon_0}{2}\frac{d}{dt}\|\mu_0\boldsymbol{H}^*\|_0^2 + \epsilon_0^2\mu_0(G\boldsymbol{E}^*, \boldsymbol{E}^*) + \epsilon_0\mu_0^2(G\boldsymbol{H}^*, \boldsymbol{H}^*) \\ = \epsilon_0\mu_0\frac{d}{dt}\left[(\boldsymbol{E}, \epsilon_0\boldsymbol{E}^*) + (\boldsymbol{H}, \mu_0\boldsymbol{H}^*)\right] + \left(\epsilon_0\mu_0(C_m\boldsymbol{E} + D\boldsymbol{J} - \boldsymbol{f}), \epsilon_0\boldsymbol{E}^*\right) \\ + \left(\epsilon_0\mu_0(C_m\boldsymbol{H} + D\boldsymbol{K} - \boldsymbol{g}), \mu_0\boldsymbol{H}^*\right). \tag{32}$$

Integrating (32) with respect to t from 0 to t and dropping the non-negative terms $\epsilon_0^2\mu_0(G\boldsymbol{E}^*, \boldsymbol{E}^*)$ and $\epsilon_0\mu_0^2(G\boldsymbol{H}^*, \boldsymbol{H}^*)$, we obtain

$$\left[\frac{\mu_0}{2}\|\epsilon_0\boldsymbol{E}^*\|_0^2(t) + \frac{\epsilon_0}{2}\|\mu_0\boldsymbol{H}^*\|_0^2(t)\right] - \left[\frac{\mu_0}{2}\|\epsilon_0\boldsymbol{E}^*\|_0^2(0) + \frac{\epsilon_0}{2}\|\mu_0\boldsymbol{H}^*\|_0^2(0)\right] \\ \leq \epsilon_0\mu_0\left[(\boldsymbol{E}, \epsilon_0\boldsymbol{E}^*)(t) + (\boldsymbol{H}, \mu_0\boldsymbol{H}^*)(t) - (\boldsymbol{E}, \epsilon_0\boldsymbol{E}^*)(0) - (\boldsymbol{H}, \mu_0\boldsymbol{H}^*)(0)\right] \\ + \int_0^t \left[\left(\epsilon_0\mu_0(C_m\boldsymbol{E} + D\boldsymbol{J} - \boldsymbol{f}), \epsilon_0\boldsymbol{E}^*\right) + \left(\epsilon_0\mu_0(C_m\boldsymbol{H} + D\boldsymbol{K} - \boldsymbol{g}), \mu_0\boldsymbol{H}^*\right)\right] dt. \tag{33}$$

Adding (27) and (33) together, we have

$$\begin{aligned}
&\frac{\epsilon_0}{2}\left(\|\boldsymbol{E}\|_0^2(t)+\|D^{1/2}\boldsymbol{J}\|_0^2(t)+\|\mu_0\boldsymbol{H}^*\|_0^2(t)\right)\\
&\quad+\frac{\mu_0}{2}\left(\|\boldsymbol{H}\|_0^2(t)+\|D^{1/2}\boldsymbol{K}\|_0^2(t)+\|\epsilon_0\boldsymbol{E}^*\|_0^2(t)\right)\\
&\quad\le\frac{\epsilon_0}{2}\left(\|\boldsymbol{E}\|_0^2(0)+\|D^{1/2}\boldsymbol{J}\|_0^2(0)+\|\mu_0\boldsymbol{H}^*\|_0^2(0)\right)\\
&\quad+\frac{\mu_0}{2}\left(\|\boldsymbol{H}\|_0^2(0)+\|D^{1/2}\boldsymbol{K}\|_0^2(0)+\|\epsilon_0\boldsymbol{E}^*\|_0^2(0)\right)\\
&\quad+\epsilon_0\mu_0\left[(\boldsymbol{E},\epsilon_0\boldsymbol{E}^*)(t)+(\boldsymbol{H},\mu_0\boldsymbol{H}^*)(t)-(\boldsymbol{E},\epsilon_0\boldsymbol{E}^*)(0)-(\boldsymbol{H},\mu_0\boldsymbol{H}^*)(0)\right]\\
&\quad+\int_0^t\Big[\left((\epsilon_0\mu_0C_m+G)\boldsymbol{E}+\epsilon_0\mu_0D\boldsymbol{J}-\epsilon_0\mu_0\boldsymbol{f},\epsilon_0\boldsymbol{E}^*\right)+\epsilon_0(\boldsymbol{f},\boldsymbol{E})\\
&\quad+\left((\epsilon_0\mu_0C_m+G)\boldsymbol{H}+\epsilon_0\mu_0D\boldsymbol{K}-\epsilon_0\mu_0\boldsymbol{g},\mu_0\boldsymbol{H}^*\right)+\mu_0(\boldsymbol{g},\boldsymbol{H})\Big]dt. \qquad (34)
\end{aligned}$$

(III) Now we need to bound those right hand terms of (34). Using the Cauchy–schwarz inequality and the definition of C_v, we have

$$\begin{aligned}
\epsilon_0\mu_0(\boldsymbol{E},\epsilon_0\boldsymbol{E}^*)(t)&=\sqrt{\epsilon_0\mu_0}(\sqrt{\epsilon_0}\boldsymbol{E},\sqrt{\mu_0}(\epsilon_0\boldsymbol{E}^*))(t)\\
&\le\frac{1}{C_v}\left[\frac{\epsilon_0}{2}\|\boldsymbol{E}\|_0^2(t)+\frac{\mu_0}{2}\|\epsilon_0\boldsymbol{E}^*\|_0^2(t)\right]. \qquad (35)
\end{aligned}$$

By the same technique, we obtain

$$\begin{aligned}
\epsilon_0\mu_0(\boldsymbol{H},\mu_0\boldsymbol{H}^*)(t)&=\sqrt{\epsilon_0\mu_0}(\sqrt{\mu_0}\boldsymbol{H},\sqrt{\epsilon_0}(\mu_0\boldsymbol{H}^*))(t)\\
&\le\frac{1}{C_v}\left[\frac{\epsilon_0}{2}\|\mu_0\boldsymbol{H}^*\|_0^2(t)+\frac{\mu_0}{2}\|\boldsymbol{H}\|_0^2(t)\right]. \qquad (36)
\end{aligned}$$

Similarly, we have

$$\begin{aligned}
\int_0^t((\epsilon_0\mu_0C_m+G)\boldsymbol{E},\epsilon_0\boldsymbol{E}^*)dt&=\int_0^t\left((\sqrt{\epsilon_0\mu_0}C_m+\frac{G}{\sqrt{\epsilon_0\mu_0}})\sqrt{\epsilon_0}\boldsymbol{E},\sqrt{\mu_0}(\epsilon_0\boldsymbol{E}^*)\right)dt\\
&\le|\frac{C_m}{C_v}+C_vG|_{L^\infty(\overline{\Omega})}\int_0^t|\left(\sqrt{\epsilon_0}\boldsymbol{E},\sqrt{\mu_0}(\epsilon_0\boldsymbol{E}^*)\right)|dt \qquad (37)\\
&\le|\frac{C_m}{C_v}+C_vG|_{L^\infty(\overline{\Omega})}\left[\int_0^t\frac{\epsilon_0}{2}\|\boldsymbol{E}\|_0^2dt+\int_0^t\frac{\mu_0}{2}\|\epsilon_0\boldsymbol{E}^*\|_0^2dt\right],\\
\int_0^t(\epsilon_0\mu_0D\boldsymbol{J},\epsilon_0\boldsymbol{E}^*)dt&=\sqrt{\epsilon_0\mu_0}\int_0^t\left(\sqrt{\epsilon_0}D\boldsymbol{J},\sqrt{\mu_0}(\epsilon_0\boldsymbol{E}^*)\right)dt \qquad (38)\\
&\le\frac{1}{C_v}\left[|D|_{L^\infty(\overline{\Omega})}\int_0^t\frac{\epsilon_0}{2}\|D^{1/2}\boldsymbol{J}\|_0^2dt+\int_0^t\frac{\mu_0}{2}\|\epsilon_0\boldsymbol{E}^*\|_0^2dt\right],\\
\int_0^t-(\epsilon_0\mu_0\boldsymbol{f},\epsilon_0\boldsymbol{E}^*)dt&=-\sqrt{\epsilon_0\mu_0}\int_0^t\left(\sqrt{\epsilon_0}\boldsymbol{f},\sqrt{\mu_0}(\epsilon_0\boldsymbol{E}^*)\right)dt \qquad (39)\\
&\le\frac{1}{C_v}\left[\int_0^t\frac{\epsilon_0}{2}\|\boldsymbol{f}\|_0^2dt+\int_0^t\frac{\mu_0}{2}\|\epsilon_0\boldsymbol{E}^*\|_0^2dt\right],
\end{aligned}$$

and

$$\int_0^t \epsilon_0(\boldsymbol{f},\boldsymbol{E})dt = \int_0^t \left(\sqrt{\epsilon_0}\boldsymbol{f}, \sqrt{\epsilon_0}\boldsymbol{E}\right)dt \le \int_0^t \frac{\epsilon_0}{2}\|\boldsymbol{f}\|_0^2 dt + \int_0^t \frac{\epsilon_0}{2}\|\boldsymbol{E}\|_0^2 dt. \quad (40)$$

By the same technique, we obtain

$$\begin{aligned}
\int_0^t ((\epsilon_0\mu_0 C_m + G)\boldsymbol{H}, \mu_0\boldsymbol{H}^*)dt &= \int_0^t \left((\sqrt{\epsilon_0\mu_0}C_m + \frac{G}{\sqrt{\epsilon_0\mu_0}})\sqrt{\mu_0}\boldsymbol{H}, \sqrt{\epsilon_0}(\mu_0\boldsymbol{H}^*)\right) dt \\
&\le |\frac{C_m}{C_v} + C_v G|_{L^\infty(\overline{\Omega})} \int_0^t \left(\sqrt{\mu_0}\boldsymbol{H}, \sqrt{\epsilon_0}(\mu_0\boldsymbol{H}^*)\right) dt \\
&\le |\frac{C_m}{C_v} + C_v G|_{L^\infty(\overline{\Omega})} \left[\int_0^t \frac{\epsilon_0}{2}\|\mu_0\boldsymbol{H}^*\|_0^2 dt + \int_0^t \frac{\mu_0}{2}\|\boldsymbol{H}\|_0^2 dt\right],
\end{aligned} \quad (41)$$

$$\begin{aligned}
\int_0^t (\epsilon_0\mu_0 D\boldsymbol{K}, \mu_0\boldsymbol{H}^*)dt &= \sqrt{\epsilon_0\mu_0}\int_0^t \left(\sqrt{\mu_0}D\boldsymbol{K}, \sqrt{\epsilon_0}(\mu_0\boldsymbol{H}^*)\right) dt \\
&\le \frac{1}{C_v}\left[|D|_{L^\infty(\overline{\Omega})}\int_0^t \frac{\mu_0}{2}\|D^{1/2}\boldsymbol{K}\|_0^2 dt + \int_0^t \frac{\epsilon_0}{2}\|\mu_0\boldsymbol{H}^*\|_0^2 dt\right],
\end{aligned} \quad (42)$$

$$\begin{aligned}
\int_0^t -(\epsilon_0\mu_0\boldsymbol{g}, \mu_0\boldsymbol{H}^*)dt &= -\sqrt{\epsilon_0\mu_0}\int_0^t \left(\sqrt{\mu_0}\boldsymbol{g}, \sqrt{\epsilon_0}(\mu_0\boldsymbol{H}^*)\right) dt \\
&\le \frac{1}{C_v}\left[\int_0^t \frac{\epsilon_0}{2}\|\mu_0\boldsymbol{H}^*\|_0^2 dt + \int_0^t \frac{\mu_0}{2}\|\boldsymbol{g}\|_0^2 dt\right],
\end{aligned} \quad (43)$$

and

$$\int_0^t \mu_0(\boldsymbol{g},\boldsymbol{H})dt = \int_0^t \left(\sqrt{\mu_0}\boldsymbol{g}, \sqrt{\mu_0}\boldsymbol{H}\right)dt \le \int_0^t \frac{\mu_0}{2}\|\boldsymbol{g}\|_0^2 dt + \int_0^t \frac{\mu_0}{2}\|\boldsymbol{H}\|_0^2 dt. \quad (44)$$

Substituting the estimates (38)–(44) into (34), and using the definitions $\mathcal{E}(t)$ and C_{stab}, we can obtain

$$(1-\frac{1}{C_v})\mathcal{E}(t) \le \mathcal{E}(0) + (1+\frac{1}{C_v})\int_0^t (\frac{\epsilon_0}{2}\|\boldsymbol{f}\|_0^2 + \frac{\mu_0}{2}\|\boldsymbol{g}\|_0^2)dt + C_{stab}\int_0^t \mathcal{E}dt,$$

which completes the proof by using the Gronwall inequality. □

3 The fully discrete finite element scheme and its analysis

To design the finite element method, we partition the physical domain Ω into a family of regular cubic (or tetrahedral) meshes T_h. We denote h_K for the diameter of element $K \in T_h$ and set the maximum mesh size $h = \max_{K\in T_h} h_K$. Depending on the regularity of the solution, an arbitrary l-th ($l \ge 1$) order Raviart-Thomas-Nédélec (RTN) finite element space on a cubic mesh can be used [16]:

$$\mathbf{V}_h = \left\{\boldsymbol{\psi}_h \in H(div;\Omega) : \psi_h\big|_K \in Q_{l,l-l,l-l} \times Q_{l-l,l,l-l} \times Q_{l-l,l-l,l}, \forall K \in T_h\right\},$$
$$\mathbf{U}_h = \left\{\boldsymbol{\phi}_h \in H(curl;\Omega) : \phi_h\big|_K \in Q_{l-l,l,l} \times Q_{l,l-l,l} \times Q_{l,l,l-l}, \forall K \in T_h\right\},$$

where $Q_{i,j,k}$ denote the space of polynomials whose degrees are less than or equal to i, j and k in variables x, y and z, respectively. To accommodate the PEC boundary condition, we denote the subspace

$$\mathbf{U}_h^0 = \left\{\boldsymbol{\phi}_h \in \mathbf{U}_h : \boldsymbol{n} \times \boldsymbol{\phi}_h = 0 \ \text{ on } \partial\Omega\right\}.$$

RTN elements on tetrahedral mesh can be defined accordingly [16].

To construct a fully discrete scheme, we divide the time interval $I = [0, T]$ into N uniform subintervals $I_i = [t_{i-1}, t_i]$ by points $t_i = i\tau, i = 0, 1, \ldots, N$, where $\tau = \frac{T}{N}$.

In practical wave simulation, the initial wave fields are usually set to zero, which makes the functions $\boldsymbol{f}$ and $\boldsymbol{g}$ in (16) and (17) zero. Hence, to simplify the rest analysis, we will ignore $\boldsymbol{f}$ and $\boldsymbol{g}$ in the PML model equatons (16)–(17).

To solve (12)–(17), we propose the following leapfrog type scheme: given initial approximations $\boldsymbol{E}_h^0, \boldsymbol{E}_h^{*0}, \boldsymbol{J}_h^0, \boldsymbol{H}_h^{\frac{1}{2}}, \boldsymbol{H}_h^{*\frac{1}{2}}, \boldsymbol{K}_h^{\frac{1}{2}}$, for any $n \geq 1$, find $\boldsymbol{E}_h^{n+1}, \boldsymbol{E}_h^{*n+1}, \boldsymbol{J}_h^{n+1} \in \mathbf{U}_h^0, \boldsymbol{H}_h^{n+\frac{3}{2}}, \boldsymbol{H}_h^{*n+\frac{3}{2}}, \boldsymbol{K}_h^{n+\frac{3}{2}} \in \mathbf{V}_h$ such that

$$\left(\epsilon_0 \frac{\boldsymbol{E}_h^{*n+1} - \boldsymbol{E}_h^{*n}}{\tau}, \boldsymbol{\Psi}_h\right) = \left(\boldsymbol{H}_h^{n+\frac{1}{2}}, \nabla \times \boldsymbol{\Psi}_h\right), \qquad \forall \boldsymbol{\Psi}_h \in \boldsymbol{U}_h^0, \tag{45}$$

$$\left(\mu_0 \frac{\boldsymbol{H}_h^{*n+\frac{3}{2}} - \boldsymbol{H}_h^{*n+\frac{1}{2}}}{\tau}, \boldsymbol{\Phi}_h\right) = -\left(\nabla \times \boldsymbol{E}_h^{n+1}, \boldsymbol{\Phi}_h\right), \qquad \forall \boldsymbol{\Phi}_h \in \boldsymbol{V}_h, \tag{46}$$

$$\left(D \frac{\boldsymbol{J}_h^{n+1} - \boldsymbol{J}_h^{n}}{\tau}, \widetilde{\boldsymbol{\Psi}}_h\right) = \left(D \frac{\boldsymbol{E}_h^{n+1} + \boldsymbol{E}_h^{n}}{2}, \widetilde{\boldsymbol{\Psi}}_h\right), \qquad \forall \widetilde{\boldsymbol{\Psi}}_h \in \boldsymbol{U}_h^0, \tag{47}$$

$$\left(D \frac{\boldsymbol{K}_h^{n+\frac{3}{2}} - \boldsymbol{K}_h^{n+\frac{1}{2}}}{\tau}, \widetilde{\boldsymbol{\Phi}}_h\right) = \left(D \frac{\boldsymbol{H}_h^{n+\frac{3}{2}} + \boldsymbol{H}_h^{n+\frac{1}{2}}}{2}, \widetilde{\boldsymbol{\Phi}}_h\right), \qquad \forall \widetilde{\boldsymbol{\Phi}}_h \in \boldsymbol{V}_h, \tag{48}$$

$$\begin{aligned}&\left(\frac{\boldsymbol{E}_h^{n+1} - \boldsymbol{E}_h^{n}}{\tau}, \widehat{\boldsymbol{\Psi}}_h\right) + \left(C_m \frac{\boldsymbol{E}_h^{n+1} + \boldsymbol{E}_h^{n}}{2}, \widehat{\boldsymbol{\Psi}}_h\right) + \left(D \frac{\boldsymbol{J}_h^{n+1} + \boldsymbol{J}_h^{n}}{2}, \widehat{\boldsymbol{\Psi}}_h\right)\\ &= \left(\frac{\boldsymbol{E}_h^{*n+1} - \boldsymbol{E}_h^{*n}}{\tau}, \widehat{\boldsymbol{\Psi}}_h\right) + \left(G \frac{\boldsymbol{E}_h^{*n+1} + \boldsymbol{E}_h^{*n}}{2}, \widehat{\boldsymbol{\Psi}}_h\right), \qquad \forall \widehat{\boldsymbol{\Psi}}_h \in \boldsymbol{U}_h^0,\end{aligned} \tag{49}$$

$$\begin{aligned}&\left(\frac{\boldsymbol{H}_h^{n+\frac{3}{2}} - \boldsymbol{H}_h^{n+\frac{1}{2}}}{\tau}, \widehat{\boldsymbol{\Phi}}_h\right) + \left(C_m \frac{\boldsymbol{H}_h^{n+\frac{3}{2}} + \boldsymbol{H}_h^{n+\frac{1}{2}}}{2}, \widehat{\boldsymbol{\Phi}}_h\right) + \left(D \frac{\boldsymbol{K}_h^{n+\frac{3}{2}} + \boldsymbol{K}_h^{n+\frac{1}{2}}}{2}, \widehat{\boldsymbol{\Phi}}_h\right)\\ &= \left(\frac{\boldsymbol{H}_h^{*n+\frac{3}{2}} - \boldsymbol{H}_h^{*n+\frac{1}{2}}}{\tau}, \widehat{\boldsymbol{\Phi}}_h\right) + \left(G \frac{\boldsymbol{H}_h^{*n+\frac{3}{2}} + \boldsymbol{H}_h^{*n+\frac{1}{2}}}{2}, \widehat{\boldsymbol{\Phi}}_h\right), \qquad \forall \widehat{\boldsymbol{\Phi}}_h \in \boldsymbol{V}_h.\end{aligned} \tag{50}$$

This scheme can be implemented as follows:

1. Update $\boldsymbol{E}_h^{*n+1}$ by solving (45) ;
2. From (47), we obtain

$$\left(D\boldsymbol{J}_h^{n+1}, \widetilde{\boldsymbol{\Psi}}_h\right) = \left(D\boldsymbol{J}_h^n, \widetilde{\boldsymbol{\Psi}}_h\right) + \tau\left(D\frac{\boldsymbol{E}_h^{n+1} + \boldsymbol{E}_h^n}{2}, \widetilde{\boldsymbol{\Psi}}_h\right).$$

   Substituting this equation into (49), we can update $\boldsymbol{E}_h^{n+1}$ by solving the new equation (49);
3. Update $\boldsymbol{J}_h^{n+1}$ by solving (47); Update $\boldsymbol{H}_h^{*n+\frac{3}{2}}$ by solving (46). Note that these two updates can be done in parallel.
4. From (48), we obtain

$$\left(D\boldsymbol{K}_h^{n+\frac{3}{2}}, \widetilde{\boldsymbol{\Phi}}_h\right) = \left(D\boldsymbol{K}_h^{n+\frac{1}{2}}, \widetilde{\boldsymbol{\Phi}}_h\right) + \tau\left(D\frac{\boldsymbol{H}_h^{n+\frac{3}{2}} + \boldsymbol{H}_h^{n+\frac{1}{2}}}{2}, \widetilde{\boldsymbol{\Phi}}_h\right).$$

   Substituting this equation into (50), we can update $\boldsymbol{H}_h^{n+\frac{3}{2}}$ by solving the updated equation (50).
5. Update $\boldsymbol{K}_h^{n+\frac{3}{2}}$ by solving (48).

3.1 The stability analysis

We dedicate this section to the stability analysis for the proposed finite element scheme (45)–(50). First, let us introduce the average the operator and central difference operator for a time sequence solution u^n:

$$\overline{u}^{n+\frac{1}{2}} = \frac{u^{n+1} + u^n}{2}, \qquad \delta_t u^{n+\frac{1}{2}} = \frac{u^{n+1} - u^n}{\tau}.$$

For the stability analysis, we need the following lemma.

Lemma 1 *For any two sequences u^n and v^n, $n = 0, 1, 2, \ldots, M+1$, we have*

$$\sum_{n=0}^{M} \overline{v}^{n+\frac{1}{2}} \delta_t u^{n+\frac{1}{2}} = \frac{1}{\tau}(u^{M+1}v^{M+1} - u^0 v^0) - \sum_{n=0}^{M} \overline{u}^{n+\frac{1}{2}} \delta_t v^{n+\frac{1}{2}}.$$

Proof It is easy to check that

$$\begin{aligned}
&\sum_{n=0}^{M} \overline{v}^{n+\frac{1}{2}} \delta_t u^{n+\frac{1}{2}} + \sum_{n=0}^{M} \overline{u}^{n+\frac{1}{2}} \delta_t v^{n+\frac{1}{2}} \\
&= \sum_{n=0}^{M} \frac{1}{2\tau}\left[(u^{n+1}v^{n+1} - u^n v^{n+1} + u^{n+1}v^n - u^n v^n) + (u^{n+1}v^{n+1} + u^n v^{n+1} - u^{n+1}v^n - u^n v^n)\right]
\end{aligned}$$

$$= \sum_{n=0}^{M} \frac{1}{\tau}(u^{n+1}v^{n+1} - u^n v^n) = \frac{1}{\tau}(u^{M+1}v^{M+1} - u^0 v^0),$$

which completes the proof. □

With the above preparations, now we can peove the following numerical stability.

Theorem 2 *Under the CFL constraint*

$$\tau \le \min\left\{\frac{h}{2C_v C_{inv}}, \ \frac{1}{2|\frac{C_m}{C_v} + C_v G|_{L^\infty(\overline{\Omega})}}\right\}, \tag{51}$$

where the positive constant C_{inv} comes from the standard inverse estimate [14,16]*:*

$$\|\nabla \times \boldsymbol{u}_h\|_0 \le C_{inv} h^{-1} \|\boldsymbol{u}_h\|_0, \quad \forall \boldsymbol{u} \in \boldsymbol{U}_h, \tag{52}$$

then the solution $\left(\boldsymbol{E}_h, \boldsymbol{H}_h, \boldsymbol{E}_h^*, \boldsymbol{H}_h^*, \boldsymbol{J}_h, \boldsymbol{K}_h\right)$ of (45)–(50) *satisfies the following stability: For any $N \ge 0$,*

$$\begin{aligned}
&\frac{\epsilon_0}{2}\left(\|\boldsymbol{E}_h^{N+1}\|_0^2 + \|D^{1/2}\boldsymbol{J}_h^{N+1}\|_0^2 + \|\mu_0 \boldsymbol{H}_h^{*N+\frac{3}{2}}\|_0^2\right) \\
&\quad + \frac{\mu_0}{2}\left(\|\boldsymbol{H}_h^{N+\frac{3}{2}}\|_0^2 + \|D^{1/2}\boldsymbol{K}_h^{N+\frac{3}{2}}\|_0^2 + \|\epsilon_0 \boldsymbol{E}_h^{*N+1}\|_0^2\right) \\
&\le C\left[\frac{\epsilon_0}{2}\left(\|\boldsymbol{E}_h^0\|_0^2 + \|D^{1/2}\boldsymbol{J}_h^0\|_0^2 + \|\mu_0 \boldsymbol{H}_h^{*\frac{1}{2}}\|_0^2\right)\right. \\
&\quad \left. + \frac{\mu_0}{2}\left(\|\boldsymbol{H}_h^{\frac{1}{2}}\|_0^2 + \|D^{1/2}\boldsymbol{K}_h^{\frac{1}{2}}\|_0^2 + \|\epsilon_0 \boldsymbol{E}_h^{*0}\|_0^2\right)\right].
\end{aligned} \tag{53}$$

where the positive constant C is independent of τ and h.

Proof Our proof follows the proof developed for the continuous stability given in Theorem 1 closely. To make the proof clearly, we partition our proof into three major parts also.

(I) Letting $\widehat{\boldsymbol{\Psi}}_h = \epsilon_0 \tau \frac{\boldsymbol{E}_h^{n+1} + \boldsymbol{E}_h^n}{2}$ in (49) and $\widehat{\boldsymbol{\Phi}}_h = \mu_0 \tau \frac{\boldsymbol{H}_h^{n+\frac{3}{2}} + \boldsymbol{H}_h^{n+\frac{1}{2}}}{2}$ in (50), respectively, we have

$$\begin{aligned}
&\frac{\epsilon_0}{2}\left(\|\boldsymbol{E}_h^{n+1}\|_0^2 - \|\boldsymbol{E}_h^n\|_0^2\right) + \epsilon_0 \tau \|C_m^{1/2} \overline{\boldsymbol{E}}_h^{n+\frac{1}{2}}\|_0^2 + \epsilon_0 \tau \left(D \overline{\boldsymbol{J}}_h^{n+\frac{1}{2}}, \overline{\boldsymbol{E}}_h^{n+\frac{1}{2}}\right) \\
&\quad = \frac{\tau}{2}\left(\epsilon_0 \delta_t \boldsymbol{E}_h^{*n+\frac{1}{2}}, \boldsymbol{E}_h^{n+1} + \boldsymbol{E}_h^n\right) + \epsilon_0 \tau \left(G \overline{\boldsymbol{E}}_h^{*n+\frac{1}{2}}, \overline{\boldsymbol{E}}_h^{n+\frac{1}{2}}\right),
\end{aligned} \tag{54}$$

and

$$\frac{\mu_0}{2}\left(\|\boldsymbol{H}_h^{n+\frac{3}{2}}\|_0^2 - \|\boldsymbol{H}_h^{n+\frac{1}{2}}\|_0^2\right) + \mu_0 \tau \|C_m^{1/2} \overline{\boldsymbol{H}}_h^{n+1}\|_0^2 + \mu_0 \tau \left(D \overline{\boldsymbol{K}}_h^{n+1}, \overline{\boldsymbol{H}}_h^{n+1}\right)$$

$$= \frac{\tau}{2}\left(\mu_0\delta_t \boldsymbol{H}_h^{*n+1}, \boldsymbol{H}_h^{n+\frac{3}{2}} + \boldsymbol{H}_h^{n+\frac{1}{2}}\right) + \mu_0\tau\left(G\overline{\boldsymbol{H}}_h^{*n+\frac{3}{2}}, \overline{\boldsymbol{H}}_h^{n+1}\right). \tag{55}$$

Letting $\widetilde{\boldsymbol{\Psi}}_h = \epsilon_0\tau\frac{\boldsymbol{J}_h^{n+1}+\boldsymbol{J}_h^n}{2}$ in (47) and $\widetilde{\boldsymbol{\Phi}}_h = \mu_0\tau\frac{\boldsymbol{K}_h^{n+\frac{3}{2}}+\boldsymbol{K}_h^{n+\frac{1}{2}}}{2}$ in (48), respectively, we have

$$\begin{aligned}\epsilon_0\tau\left(D\overline{\boldsymbol{J}}_h^{n+\frac{1}{2}}, \overline{\boldsymbol{E}}_h^{n+\frac{1}{2}}\right) &= \frac{\epsilon_0}{2}\left(D(\boldsymbol{J}_h^{n+1} - \boldsymbol{J}_h^n), \boldsymbol{J}_h^{n+1} + \boldsymbol{J}_h^n\right)\\ &= \frac{\epsilon_0}{2}\left(\|D^{1/2}\boldsymbol{J}_h^{n+1}\|_0^2 - \|D^{1/2}\boldsymbol{J}_h^n\|_0^2\right),\end{aligned} \tag{56}$$

and

$$\begin{aligned}\mu_0\tau\left(D\overline{\boldsymbol{K}}_h^{n+1}, \overline{\boldsymbol{H}}_h^{n+1}\right) &= \frac{\mu_0}{2}\left(D(\boldsymbol{K}_h^{n+\frac{3}{2}} - \boldsymbol{K}_h^{n+\frac{1}{2}}), \boldsymbol{K}_h^{n+\frac{3}{2}} + \boldsymbol{K}_h^{n+\frac{1}{2}}\right)\\ &= \frac{\mu_0}{2}\left(\|D^{1/2}\boldsymbol{K}_h^{n+\frac{3}{2}}\|_0^2 - \|D^{1/2}\boldsymbol{K}_h^{n+\frac{1}{2}}\|_0^2\right).\end{aligned} \tag{57}$$

Choosing $\boldsymbol{\Psi}_h = \tau\frac{\boldsymbol{E}_h^{n+1}+\boldsymbol{E}_h^n}{2}$ in (45) and $\boldsymbol{\Phi}_h = \tau\frac{\boldsymbol{H}_h^{n+\frac{3}{2}}+\boldsymbol{H}_h^{n+\frac{1}{2}}}{2}$ in (46), respectively, we have

$$\frac{\tau}{2}\left(\epsilon_0\delta_t\boldsymbol{E}_h^{*n+\frac{1}{2}}, \boldsymbol{E}_h^{n+1} + \boldsymbol{E}_h^n\right) = \frac{\tau}{2}\left(\boldsymbol{H}_h^{n+\frac{1}{2}}, \nabla\times(\boldsymbol{E}_h^{n+1} + \boldsymbol{E}_h^n)\right), \tag{58}$$

and

$$\frac{\tau}{2}\left(\mu_0\delta_t\boldsymbol{H}_h^{*n+1}, \boldsymbol{H}_h^{n+\frac{3}{2}} + \boldsymbol{H}_h^{n+\frac{1}{2}}\right) = -\frac{\tau}{2}\left(\nabla\times\boldsymbol{E}_h^{n+1}, \boldsymbol{H}_h^{n+\frac{3}{2}} + \boldsymbol{H}_h^{n+\frac{1}{2}}\right). \tag{59}$$

Adding (54) and (55) together, and substituting (56)–(59) into the reult, we obtain

$$\begin{aligned}&\left[\frac{\epsilon_0}{2}\left(\|\boldsymbol{E}_h^{n+1}\|_0^2 + \|D^{1/2}\boldsymbol{J}_h^{n+1}\|_0^2\right) + \frac{\mu_0}{2}\left(\|\boldsymbol{H}_h^{n+\frac{3}{2}}\|_0^2 + \|D^{1/2}\boldsymbol{K}_h^{n+\frac{3}{2}}\|_0^2\right)\right]\\ &\quad - \left[\frac{\epsilon_0}{2}\left(\|\boldsymbol{E}_h^n\|_0^2 + \|D^{1/2}\boldsymbol{J}_h^n\|_0^2\right) + \frac{\mu_0}{2}\left(\|\boldsymbol{H}_h^{n+\frac{1}{2}}\|_0^2 + \|D^{1/2}\boldsymbol{K}_h^{n+\frac{1}{2}}\|_0^2\right)\right]\\ &\quad + \epsilon_0\tau\|C_m^{1/2}\overline{\boldsymbol{E}}_h^{n+\frac{1}{2}}\|_0^2 + \mu_0\tau\|C_m^{1/2}\overline{\boldsymbol{H}}_h^{n+1}\|_0^2\\ &= \frac{\tau}{2}\left[\left(\boldsymbol{H}_h^{n+\frac{1}{2}}, \nabla\times(\boldsymbol{E}_h^{n+1} + \boldsymbol{E}_h^n)\right) - \left(\nabla\times\boldsymbol{E}_h^{n+1}, \boldsymbol{H}_h^{n+\frac{3}{2}} + \boldsymbol{H}_h^{n+\frac{1}{2}}\right)\right]\\ &\quad + \epsilon_0\tau\left(G\overline{\boldsymbol{E}}_h^{*n+\frac{1}{2}}, \overline{\boldsymbol{E}}_h^{n+\frac{1}{2}}\right) + \mu_0\tau\left(G\overline{\boldsymbol{H}}_h^{*n+1}, \overline{\boldsymbol{H}}_h^{n+1}\right).\end{aligned} \tag{60}$$

It is easy to check that

$$\frac{\tau}{2}\left[\left(\boldsymbol{H}_h^{n+\frac{1}{2}}, \nabla\times(\boldsymbol{E}_h^{n+1}+\boldsymbol{E}_h^{n})\right)-\left(\nabla\times\boldsymbol{E}_h^{n+1}, \boldsymbol{H}_h^{n+\frac{3}{2}}+\boldsymbol{H}_h^{n+\frac{1}{2}}\right)\right]$$
$$=\frac{\tau}{2}\left[\left(\nabla\times\boldsymbol{E}_h^{n}, \boldsymbol{H}_h^{n+\frac{1}{2}}\right)-\left(\nabla\times\boldsymbol{E}_h^{n+1}, \boldsymbol{H}_h^{n+\frac{3}{2}}\right)\right]. \quad (61)$$

Substituting (61) into (60), dropping the non-negative terms $\epsilon_0\tau\|C_m^{1/2}\overline{\boldsymbol{E}}_h^{n+\frac{1}{2}}\|_0^2$ and $\mu_0\tau\|C_m^{1/2}\overline{\boldsymbol{H}}_h^{n+1}\|_0^2$ and summing up the result from $n=0$ to N, we have

$$\frac{\epsilon_0}{2}\left(\|\boldsymbol{E}_h^{N+1}\|_0^2+\|D^{1/2}\boldsymbol{J}_h^{N+1}\|_0^2\right)+\frac{\mu_0}{2}\left(\|\boldsymbol{H}_h^{N+\frac{3}{2}}\|_0^2+\|D^{1/2}\boldsymbol{K}_h^{N+\frac{3}{2}}\|_0^2\right)$$
$$\leq\frac{\epsilon_0}{2}\left(\|\boldsymbol{E}_h^{0}\|_0^2+\|D^{1/2}\boldsymbol{J}_h^{0}\|_0^2\right)+\frac{\mu_0}{2}\left(\|\boldsymbol{H}_h^{\frac{1}{2}}\|_0^2+\|D^{1/2}\boldsymbol{K}_h^{\frac{1}{2}}\|_0^2\right)$$
$$+\frac{\tau}{2}\left[\left(\nabla\times\boldsymbol{E}_h^{0}, \boldsymbol{H}_h^{\frac{1}{2}}\right)-\left(\nabla\times\boldsymbol{E}_h^{N+1}, \boldsymbol{H}_h^{N+\frac{3}{2}}\right)\right]$$
$$+\sum_{n=0}^{N}\tau\left(G\overline{\boldsymbol{E}}_h^{n+\frac{1}{2}}, \epsilon_0\overline{\boldsymbol{E}}_h^{*n+\frac{1}{2}}\right)+\sum_{n=0}^{N}\tau\left(G\overline{\boldsymbol{H}}_h^{n+1}, \mu_0\overline{\boldsymbol{H}}_h^{*n+1}\right). \quad (62)$$

(II) To bound $\boldsymbol{E}_h^*$ and $\boldsymbol{H}_h^*$ in (62), we follow the similar technique developed in the continuous case. Letting $\widehat{\boldsymbol{\Psi}}_h=\epsilon_0^2\mu_0\tau\frac{\boldsymbol{E}_h^{*n+1}+\boldsymbol{E}_h^{*n}}{2}$ in (49) and $\widehat{\boldsymbol{\Phi}}_h=\epsilon_0\mu_0^2\tau\frac{\boldsymbol{H}_h^{*n+\frac{3}{2}}+\boldsymbol{H}_h^{*n+\frac{1}{2}}}{2}$ in (50), respectively, we have

$$\frac{\mu_0}{2}\left(\|\epsilon_0\boldsymbol{E}_h^{*n+1}\|_0^2-\|\epsilon_0\boldsymbol{E}_h^{*n}\|_0^2\right)+\mu_0\tau\|G^{1/2}\epsilon_0\overline{\boldsymbol{E}}_h^{*n+\frac{1}{2}}\|_0^2$$
$$=\tau\epsilon_0\mu_0\left[\left(\delta_t\boldsymbol{E}_h^{n+\frac{1}{2}}, \epsilon_0\overline{\boldsymbol{E}}_h^{*n+\frac{1}{2}}\right)+\left(C_m\overline{\boldsymbol{E}}_h^{n+\frac{1}{2}}, \epsilon_0\overline{\boldsymbol{E}}_h^{*n+\frac{1}{2}}\right)+\left(D\overline{\boldsymbol{J}}_h^{n+\frac{1}{2}}, \epsilon_0\overline{\boldsymbol{E}}_h^{*n+\frac{1}{2}}\right)\right], \quad (63)$$

and

$$\frac{\epsilon_0}{2}\left(\|\mu_0\boldsymbol{H}_h^{*n+\frac{3}{2}}\|_0^2-\|\mu_0\boldsymbol{H}_h^{*n+\frac{1}{2}}\|_0^2\right)+\epsilon_0\tau\|G^{1/2}\mu_0\overline{\boldsymbol{H}}_h^{*n+1}\|_0^2$$
$$=\tau\epsilon_0\mu_0\left[\left(\delta_t\boldsymbol{H}_h^{n+1}, \mu_0\overline{\boldsymbol{H}}_h^{*n+1}\right)+\left(C_m\overline{\boldsymbol{H}}_h^{n+1}, \mu_0\overline{\boldsymbol{H}}_h^{*n+1}\right)+\left(D\overline{\boldsymbol{K}}_h^{n+1}, \mu_0\overline{\boldsymbol{H}}_h^{*n+1}\right)\right]. \quad (64)$$

Adding (63) and (64) together, dropping the non-negative terms $\mu_0\tau\|G^{1/2}\epsilon_0\overline{\boldsymbol{E}}_h^{*n+\frac{1}{2}}\|_0^2$ and $\epsilon_0\tau\|G^{1/2}\mu_0\overline{\boldsymbol{H}}_h^{*n+1}\|_0^2$, and summing up the result from $n=0$ to N, we have

$$\left(\frac{\epsilon_0}{2}\|\mu_0\boldsymbol{H}_h^{*N+\frac{3}{2}}\|_0^2+\frac{\mu_0}{2}\|\epsilon_0\boldsymbol{E}_h^{*N+1}\|_0^2\right)-\left(\frac{\epsilon_0}{2}\|\mu_0\boldsymbol{H}_h^{*\frac{1}{2}}\|_0^2+\frac{\mu_0}{2}\|\epsilon_0\boldsymbol{E}_h^{*0}\|_0^2\right)$$

$$\leq \tau\epsilon_0\mu_0 \sum_{n=0}^{N} \left[\left(\delta_t \boldsymbol{E}_h^{n+\frac{1}{2}}, \epsilon_0 \overline{\boldsymbol{E}}_h^{*n+\frac{1}{2}} \right) + \left(\delta_t \boldsymbol{H}_h^{n+1}, \mu_0 \overline{\boldsymbol{H}}_h^{*n+1} \right) \right]$$
$$+ \tau \sum_{n=0}^{N} \epsilon_0\mu_0 \left[\left(C_m \overline{\boldsymbol{E}}_h^{n+\frac{1}{2}} + D\overline{\boldsymbol{J}}_h^{n+\frac{1}{2}}, \epsilon_0 \overline{\boldsymbol{E}}_h^{*n+\frac{1}{2}} \right) + \left(C_m \overline{\boldsymbol{H}}_h^{n+1} + D\overline{\boldsymbol{K}}_h^{n+1}, \mu_0 \overline{\boldsymbol{H}}_h^{*n+1} \right) \right]. \tag{65}$$

Using Lemma 1, we have

$$\tau\epsilon_0\mu_0 \sum_{n=0}^{N} \left(\delta_t \boldsymbol{E}_h^{n+\frac{1}{2}}, \epsilon_0 \overline{\boldsymbol{E}}_h^{*n+\frac{1}{2}} \right) = \epsilon_0\mu_0 \left[\left(\boldsymbol{E}_h^{N+1}, \epsilon_0 \boldsymbol{E}_h^{*N+1} \right) - \left(\boldsymbol{E}_h^0, \epsilon_0 \boldsymbol{E}_h^{*0} \right) \right]$$
$$- \tau\epsilon_0\mu_0 \sum_{n=0}^{N} \left(\overline{\boldsymbol{E}}_h^{n+\frac{1}{2}}, \epsilon_0 \delta_t \boldsymbol{E}_h^{*n+\frac{1}{2}} \right), \tag{66}$$

and

$$\tau\epsilon_0\mu_0 \sum_{n=0}^{N} \left(\delta_t \boldsymbol{H}_h^{n+1}, \mu_0 \overline{\boldsymbol{H}}_h^{*n+1} \right) = \epsilon_0\mu_0 \left[\left(\boldsymbol{H}_h^{N+\frac{3}{2}}, \mu_0 \boldsymbol{H}_h^{*N+\frac{3}{2}} \right) - \left(\boldsymbol{H}_h^{\frac{1}{2}}, \mu_0 \boldsymbol{H}_h^{*\frac{1}{2}} \right) \right]$$
$$- \tau\epsilon_0\mu_0 \sum_{n=0}^{N} \left(\overline{\boldsymbol{H}}_h^{n+1}, \mu_0 \delta_t \boldsymbol{H}_h^{*n+1} \right). \tag{67}$$

Adding (66) and (67) together, using (58), (59) and (61), we have

$$\tau\epsilon_0\mu_0 \sum_{n=0}^{N} \left[\left(\delta_t \boldsymbol{E}_h^{n+\frac{1}{2}}, \epsilon_0 \overline{\boldsymbol{E}}_h^{*n+\frac{1}{2}} \right) + \left(\delta_t \boldsymbol{H}_h^{n+1}, \mu_0 \overline{\boldsymbol{H}}_h^{*n+1} \right) \right]$$
$$= \epsilon_0\mu_0 \left[\left(\boldsymbol{E}_h^{N+1}, \epsilon_0 \boldsymbol{E}_h^{*N+1} \right) + \left(\boldsymbol{H}_h^{N+\frac{3}{2}}, \mu_0 \boldsymbol{H}_h^{*N+\frac{3}{2}} \right) - \left(\boldsymbol{E}_h^0, \epsilon_0 \boldsymbol{E}_h^{*0} \right) - \left(\boldsymbol{H}_h^{\frac{1}{2}}, \mu_0 \boldsymbol{H}_h^{*\frac{1}{2}} \right) \right]$$
$$- \epsilon_0\mu_0 \sum_{n=0}^{N} \left[\tau \left(\overline{\boldsymbol{E}}_h^{n+\frac{1}{2}}, \epsilon_0 \delta_t \boldsymbol{E}_h^{*n+\frac{1}{2}} \right) + \tau \left(\overline{\boldsymbol{H}}_h^{n+1}, \mu_0 \delta_t \boldsymbol{H}_h^{*n+1} \right) \right] \tag{68}$$
$$= \epsilon_0\mu_0 \left[\left(\boldsymbol{E}_h^{N+1}, \epsilon_0 \boldsymbol{E}_h^{*N+1} \right) + \left(\boldsymbol{H}_h^{N+\frac{3}{2}}, \mu_0 \boldsymbol{H}_h^{*N+\frac{3}{2}} \right) - \left(\boldsymbol{E}_h^0, \epsilon_0 \boldsymbol{E}_h^{*0} \right) - \left(\boldsymbol{H}_h^{\frac{1}{2}}, \mu_0 \boldsymbol{H}_h^{*\frac{1}{2}} \right) \right]$$
$$- \epsilon_0\mu_0 \sum_{n=0}^{N} \frac{\tau}{2} \left[\left(\nabla \times \boldsymbol{E}_h^n, \boldsymbol{H}_h^{n+\frac{1}{2}} \right) - \left(\nabla \times \boldsymbol{E}_h^{n+1}, \boldsymbol{H}_h^{n+\frac{3}{2}} \right) \right]$$
$$= \epsilon_0\mu_0 \left[\left(\boldsymbol{E}_h^{N+1}, \epsilon_0 \boldsymbol{E}_h^{*N+1} \right) + \left(\boldsymbol{H}_h^{N+\frac{3}{2}}, \mu_0 \boldsymbol{H}_h^{*N+\frac{3}{2}} \right) - \left(\boldsymbol{E}_h^0, \epsilon_0 \boldsymbol{E}_h^{*0} \right) - \left(\boldsymbol{H}_h^{\frac{1}{2}}, \mu_0 \boldsymbol{H}_h^{*\frac{1}{2}} \right) \right]$$
$$+ \frac{\tau\epsilon_0\mu_0}{2} \left[\left(\nabla \times \boldsymbol{E}_h^{N+1}, \boldsymbol{H}_h^{N+\frac{3}{2}} \right) - \left(\nabla \times \boldsymbol{E}_h^0, \boldsymbol{H}_h^{\frac{1}{2}} \right) \right].$$

Substituting (68) into (65) and adding the result with (62), we have

$$\frac{\epsilon_0}{2} \left(\|\boldsymbol{E}_h^{N+1}\|_0^2 + \|D^{1/2} \boldsymbol{J}_h^{N+1}\|_0^2 + \|\mu_0 \boldsymbol{H}_h^{*N+\frac{3}{2}}\|_0^2 \right)$$

$$
\begin{aligned}
&+\frac{\mu_0}{2}\left(\|\boldsymbol{H}_h^{N+\frac{3}{2}}\|_0^2+\|D^{1/2}\boldsymbol{K}_h^{N+\frac{3}{2}}\|_0^2+\|\epsilon_0\boldsymbol{E}_h^{*N+1}\|_0^2\right)\\
&\le\frac{\epsilon_0}{2}\left(\|\boldsymbol{E}_h^{0}\|_0^2+\|D^{1/2}\boldsymbol{J}_h^{0}\|_0^2+\|\mu_0\boldsymbol{H}_h^{*\frac{1}{2}}\|_0^2\right)\\
&+\frac{\mu_0}{2}\left(\|\boldsymbol{H}_h^{\frac{1}{2}}\|_0^2+\|D^{1/2}\boldsymbol{K}_h^{\frac{1}{2}}\|_0^2+\|\epsilon_0\boldsymbol{E}_h^{*0}\|_0^2\right)\\
&-\left(\frac{\tau}{2}-\frac{\tau\epsilon_0\mu_0}{2}\right)\left[\left(\nabla\times\boldsymbol{E}_h^{N+1},\boldsymbol{H}_h^{N+\frac{3}{2}}\right)-\left(\nabla\times\boldsymbol{E}_h^{0},\boldsymbol{H}_h^{\frac{1}{2}}\right)\right]\\
&+\epsilon_0\mu_0\left[\left(\boldsymbol{E}_h^{N+1},\epsilon_0\boldsymbol{E}_h^{*N+1}\right)+\left(\boldsymbol{H}_h^{N+\frac{3}{2}},\mu_0\boldsymbol{H}_h^{*N+\frac{3}{2}}\right)-\left(\boldsymbol{E}_h^{0},\epsilon_0\boldsymbol{E}_h^{*0}\right)\right.\\
&\left.-\left(\boldsymbol{H}_h^{\frac{1}{2}},\mu_0\boldsymbol{H}_h^{*\frac{1}{2}}\right)\right]\\
&+\tau\sum_{n=0}^{N}\left((\epsilon_0\mu_0C_m+G)\overline{\boldsymbol{E}}_h^{n+\frac{1}{2}}+\epsilon_0\mu_0D\overline{\boldsymbol{J}}_h^{n+\frac{1}{2}},\epsilon_0\overline{\boldsymbol{E}}_h^{*n+\frac{1}{2}}\right)\\
&+\tau\sum_{n=0}^{N}\left((\epsilon_0\mu_0C_m+G)\overline{\boldsymbol{H}}_h^{n+1}+\epsilon_0\mu_0D\overline{\boldsymbol{K}}_h^{n+1},\mu_0\overline{\boldsymbol{H}}_h^{*n+1}\right). \qquad (69)
\end{aligned}
$$

(III) Now we need to bound those right hand side terms of (69). By the inverse estimate (52) and the Cauchy–Schwarz inequality, we have

$$
\begin{aligned}
-\left(\frac{\tau}{2}-\frac{\tau\epsilon_0\mu_0}{2}\right)\left(\nabla\times\boldsymbol{E}_h^{N+1},\boldsymbol{H}_h^{N+\frac{3}{2}}\right)&\le\left(\frac{\tau C_v}{2}-\frac{\tau}{2C_v}\right)\frac{C_{inv}}{h}\cdot\sqrt{\epsilon_0}\|\boldsymbol{E}_h^{N+1}\|_0\cdot\sqrt{\mu_0}\|\boldsymbol{H}_h^{N+\frac{3}{2}}\|_0\\
&\le\left(\frac{\tau C_vC_{inv}}{2h}-\frac{\tau C_{inv}}{2hC_v}\right)\left(\frac{\epsilon_0}{2}\|\boldsymbol{E}_h^{N+1}\|_0^2+\frac{\mu_0}{2}\|\boldsymbol{H}_h^{N+\frac{3}{2}}\|_0^2\right), \qquad (70)
\end{aligned}
$$

and

$$
\begin{aligned}
\left(\frac{\tau}{2}-\frac{\tau\epsilon_0\mu_0}{2}\right)\left(\nabla\times\boldsymbol{E}_h^{0},\boldsymbol{H}_h^{\frac{1}{2}}\right)&\le\left(\frac{\tau C_v}{2}-\frac{\tau}{2C_v}\right)\frac{C_{inv}}{h}\cdot\sqrt{\epsilon_0}\|\boldsymbol{E}_h^{0}\|_0\cdot\sqrt{\mu_0}\|\boldsymbol{H}_h^{\frac{1}{2}}\|_0\\
&\le\left(\frac{\tau C_vC_{inv}}{2h}-\frac{\tau C_{inv}}{2hC_v}\right)\left(\frac{\epsilon_0}{2}\|\boldsymbol{E}_h^{0}\|_0^2+\frac{\mu_0}{2}\|\boldsymbol{H}_h^{\frac{1}{2}}\|_0^2\right). \qquad (71)
\end{aligned}
$$

Using the Cauchy–Schwarz inequality, we have

$$
\begin{aligned}
\epsilon_0\mu_0\left(\boldsymbol{E}_h^{N+1},\epsilon_0\boldsymbol{E}_h^{*N+1}\right)&\le\frac{1}{C_v}\sqrt{\epsilon_0}\|\boldsymbol{E}_h^{N+1}\|_0\cdot\sqrt{\mu_0}\|\epsilon_0\boldsymbol{E}_h^{*N+1}\|_0\\
&\le\frac{1}{C_v}\left(\frac{\epsilon_0}{2}\|\boldsymbol{E}_h^{N+1}\|_0^2+\frac{\mu_0}{2}\|\epsilon_0\boldsymbol{E}_h^{*N+1}\|_0^2\right), \qquad (72)
\end{aligned}
$$

$$\epsilon_0\mu_0\left(\boldsymbol{H}_h^{N+\frac{3}{2}}, \mu_0\boldsymbol{H}_h^{*N+\frac{3}{2}}\right) \le \frac{1}{C_v}\sqrt{\epsilon_0}\|\mu_0\boldsymbol{H}_h^{*N+\frac{3}{2}}\|_0 \cdot \sqrt{\mu_0}\|\boldsymbol{H}_h^{N+\frac{3}{2}}\|_0$$
$$\le \frac{1}{C_v}\left(\frac{\epsilon_0}{2}\|\mu_0\boldsymbol{H}_h^{*N+\frac{3}{2}}\|_0^2 + \frac{\mu_0}{2}\|\boldsymbol{H}_h^{N+\frac{3}{2}}\|_0^2\right), \tag{73}$$
$$-\epsilon_0\mu_0\left(\boldsymbol{E}_h^0, \epsilon_0\boldsymbol{E}_h^{*0}\right) \le \frac{1}{C_v}\sqrt{\epsilon_0}\|\boldsymbol{E}_h^0\|_0 \cdot \sqrt{\mu_0}\|\epsilon_0\boldsymbol{E}_h^{*0}\|_0$$
$$\le \frac{1}{C_v}\left(\frac{\epsilon_0}{2}\|\boldsymbol{E}_h^0\|_0^2 + \frac{\mu_0}{2}\|\epsilon_0\boldsymbol{E}_h^{*0}\|_0^2\right), \tag{74}$$

and

$$-\epsilon_0\mu_0\left(\boldsymbol{H}_h^{\frac{1}{2}}, \mu_0\boldsymbol{H}_h^{*\frac{1}{2}}\right) \le \frac{1}{C_v}\sqrt{\epsilon_0}\|\mu_0\boldsymbol{H}_h^{*\frac{1}{2}}\|_0 \cdot \sqrt{\mu_0}\|\boldsymbol{H}_h^{\frac{1}{2}}\|_0$$
$$\le \frac{1}{C_v}\left(\frac{\epsilon_0}{2}\|\mu_0\boldsymbol{H}_h^{*\frac{1}{2}}\|_0^2 + \frac{\mu_0}{2}\|\boldsymbol{H}_h^{\frac{1}{2}}\|_0^2\right). \tag{75}$$

Similarly, we have

$$\tau\sum_{n=0}^{N}\left((\epsilon_0\mu_0 C_m + G)\overline{\boldsymbol{E}}_h^{n+\frac{1}{2}}, \epsilon_0\overline{\boldsymbol{E}}_h^{*n+\frac{1}{2}}\right) \le \tau\sum_{n=0}^{N}|\frac{C_m}{C_v} + C_v G|_{L^\infty(\overline{\Omega})}\sqrt{\epsilon_0}\left\|\overline{\boldsymbol{E}}_h^{n+\frac{1}{2}}\right\|_0 \cdot \sqrt{\mu_0}\left\|\epsilon_0\overline{\boldsymbol{E}}_h^{*n+\frac{1}{2}}\right\|_0$$
$$\le \tau\sum_{n=0}^{N}|\frac{C_m}{C_v} + C_v G|_{L^\infty(\overline{\Omega})}\left(\frac{\epsilon_0}{2}\left\|\overline{\boldsymbol{E}}_h^{n+\frac{1}{2}}\right\|_0^2 + \frac{\mu_0}{2}\left\|\epsilon_0\overline{\boldsymbol{E}}_h^{*n+\frac{1}{2}}\right\|_0^2\right)$$
$$\le \tau\sum_{n=0}^{N}|\frac{C_m}{C_v} + C_v G|_{L^\infty(\overline{\Omega})}\left(\frac{\epsilon_0}{4}\|\boldsymbol{E}_h^{n+1}\|_0^2 + \frac{\epsilon_0}{4}\|\boldsymbol{E}_h^{n}\|_0^2 + \frac{\mu_0}{4}\|\epsilon_0\boldsymbol{E}_h^{*n+1}\|_0^2 + \frac{\mu_0}{4}\|\epsilon_0\boldsymbol{E}_h^{*n}\|_0^2\right)$$
$$\le \tau|\frac{C_m}{2C_v} + \frac{C_v G}{2}|_{L^\infty(\overline{\Omega})}\left(\frac{\epsilon_0}{2}\|\boldsymbol{E}_h^{N+1}\|_0^2 + \frac{\mu_0}{2}\|\epsilon_0\boldsymbol{E}_h^{*N+1}\|_0^2\right)$$
$$+ \tau\sum_{n=0}^{N}|\frac{C_m}{C_v} + C_v G|_{L^\infty(\overline{\Omega})}\left(\frac{\epsilon_0}{2}\|\boldsymbol{E}_h^{n}\|_0^2 + \frac{\mu_0}{2}\|\epsilon_0\boldsymbol{E}_h^{*n}\|_0^2\right), \tag{76}$$
$$\tau\sum_{n=0}^{N}\left(\epsilon_0\mu_0 D\overline{\boldsymbol{J}}_h^{n+\frac{1}{2}}, \epsilon_0\overline{\boldsymbol{E}}_h^{*n+\frac{1}{2}}\right) \le \frac{\tau}{C_v}\sum_{n=0}^{N}\sqrt{\epsilon_0}\left\|D\overline{\boldsymbol{J}}_h^{n+\frac{1}{2}}\right\|_0 \cdot \sqrt{\mu_0}\left\|\epsilon_0\overline{\boldsymbol{E}}_h^{*n+\frac{1}{2}}\right\|_0$$
$$\le \frac{\tau}{C_v}\sum_{n=0}^{N}\left(|D|_{L^\infty(\overline{\Omega})}\frac{\epsilon_0}{2}\left\|D^{1/2}\overline{\boldsymbol{J}}_h^{n+\frac{1}{2}}\right\|_0^2 + \frac{\mu_0}{2}\left\|\epsilon_0\overline{\boldsymbol{E}}_h^{*n+\frac{1}{2}}\right\|_0^2\right)$$
$$\le \frac{\tau}{2C_v}\sum_{n=0}^{N}\left(|D|_{L^\infty(\overline{\Omega})}\frac{\epsilon_0}{2}\|D^{1/2}\boldsymbol{J}_h^{n+1}\|_0^2 + |D|_{L^\infty(\overline{\Omega})}\frac{\epsilon_0}{2}\|D^{1/2}\boldsymbol{J}_h^{n}\|_0^2 + \frac{\mu_0}{2}\|\epsilon_0\boldsymbol{E}_h^{*n+1}\|_0^2 + \frac{\mu_0}{2}\|\epsilon_0\boldsymbol{E}_h^{*n}\|_0^2\right)$$
$$\le \frac{\tau}{2C_v}\left(|D|_{L^\infty(\overline{\Omega})}\frac{\epsilon_0}{2}\|D^{1/2}\boldsymbol{J}_h^{N+1}\|_0^2 + \frac{\mu_0}{2}\|\epsilon_0\boldsymbol{E}_h^{*N+1}\|_0^2\right)$$
$$+ \frac{\tau}{C_v}\sum_{n=0}^{N}\left(|D|_{L^\infty(\overline{\Omega})}\frac{\epsilon_0}{2}\|D^{1/2}\boldsymbol{J}_h^{n}\|_0^2 + \frac{\mu_0}{2}\|\epsilon_0\boldsymbol{E}_h^{*n}\|_0^2\right). \tag{77}$$

By the same technique, we can obtain

$$\tau\sum_{n=0}^{N}\left((\epsilon_0\mu_0 C_m + G)\overline{\boldsymbol{H}}_h^{n+1}, \epsilon_0\overline{\boldsymbol{H}}_h^{*n+1}\right) \le \tau\sum_{n=0}^{N}|\frac{C_m}{C_v} + GC_v|_{L^\infty(\overline{\Omega})}$$

$$
\begin{aligned}
&\cdot\sqrt{\epsilon_0}\left\|\overline{\boldsymbol{H}}_h^{n+1}\right\|_0\cdot\sqrt{\mu_0}\left\|\epsilon_0\overline{\boldsymbol{H}}_h^{*n+1}\right\|_0\\
&\le\tau|\frac{C_m}{2C_v}+\frac{GC_v}{2}|_{L^\infty(\overline{\Omega})}\left(\frac{\mu_0}{2}\|\boldsymbol{H}_h^{N+\frac{3}{2}}\|_0^2+\frac{\epsilon_0}{2}\|\mu_0\boldsymbol{H}_h^{*N+\frac{3}{2}}\|_0^2\right)\\
&+\tau\sum_{n=0}^{N}|\frac{C_m}{C_v}+GC_v|_{L^\infty(\overline{\Omega})}\left(\frac{\epsilon_0}{2}\|\mu_0\boldsymbol{H}_h^{*n+\frac{1}{2}}\|_0^2+\frac{\mu_0}{2}\|\boldsymbol{H}_h^{n+\frac{1}{2}}\|_0^2\right),
\end{aligned}
\tag{78}
$$

and

$$
\begin{aligned}
&\tau\sum_{n=0}^{N}\left(\epsilon_0\mu_0 D\overline{\boldsymbol{K}}_h^{n+1},\mu_0\overline{\boldsymbol{H}}_h^{*n+1}\right)\\
&\le\frac{\tau}{C_v}\sum_{n=0}^{N}\sqrt{\mu_0}\left\|D\overline{\boldsymbol{K}}_h^{n+1}\right\|_0\cdot\sqrt{\epsilon_0}\left\|\mu_0\overline{\boldsymbol{H}}_h^{*n+1}\right\|_0\\
&\le\frac{\tau}{2C_v}\left(|D|_{L^\infty(\overline{\Omega})}\frac{\mu_0}{2}\|D^{1/2}\boldsymbol{K}_h^{N+\frac{3}{2}}\|_0^2+\frac{\epsilon_0}{2}\|\mu_0\boldsymbol{H}_h^{*N+\frac{3}{2}}\|_0^2\right)\\
&+\frac{\tau}{C_v}\sum_{n=0}^{N}\left(|D|_{L^\infty(\overline{\Omega})}\frac{\mu_0}{2}\|D^{1/2}\boldsymbol{K}_h^{n+\frac{1}{2}}\|_0^2+\frac{\epsilon_0}{2}\|\mu_0\boldsymbol{H}_h^{*n+\frac{1}{2}}\|_0^2\right).
\end{aligned}
\tag{79}
$$

Substituting the above estimates (70)–(79) into (69), we have

$$
\begin{aligned}
&\frac{\epsilon_0}{2}\left(\|\boldsymbol{E}_h^{N+1}\|_0^2+\|D^{1/2}\boldsymbol{J}_h^{N+1}\|_0^2+\|\mu_0\boldsymbol{H}_h^{*N+\frac{3}{2}}\|_0^2\right)\\
&+\frac{\mu_0}{2}\left(\|\boldsymbol{H}_h^{N+\frac{3}{2}}\|_0^2+\|D^{1/2}\boldsymbol{K}_h^{N+\frac{3}{2}}\|_0^2+\|\epsilon_0\boldsymbol{E}_h^{*N+1}\|_0^2\right)\\
&\le\left[1+\left(\frac{\tau C_vC_{inv}}{2h}-\frac{\tau C_{inv}}{2hC_v}\right)+\frac{1}{C_v}\right]\frac{\epsilon_0}{2}\left(\|\boldsymbol{E}_h^0\|_0^2+\|D^{1/2}\boldsymbol{J}_h^0\|_0^2+\|\mu_0\boldsymbol{H}_h^{*\frac{1}{2}}\|_0^2\right)\\
&\left[1+\left(\frac{\tau C_vC_{inv}}{2h}-\frac{\tau C_{inv}}{2hC_v}\right)+\frac{1}{C_v}\right]\frac{\mu_0}{2}\left(\|\boldsymbol{H}_h^{\frac{1}{2}}\|_0^2+\|D^{1/2}\boldsymbol{K}_h^{\frac{1}{2}}\|_0^2+\|\epsilon_0\boldsymbol{E}_h^{*0}\|_0^2\right)\\
&+\left[\left(\frac{\tau C_vC_{inv}}{2h}-\frac{\tau C_{inv}}{2hC_v}\right)+\frac{1}{C_v}+\tau|\frac{C_m}{2C_v}+\frac{GC_v}{2}|_{L^\infty(\overline{\Omega})}\right]\left(\frac{\epsilon_0}{2}\|\boldsymbol{E}_h^{N+1}\|_0^2+\frac{\mu_0}{2}\|\boldsymbol{H}_h^{N+\frac{3}{2}}\|_0^2\right)\\
&+\frac{\tau}{2C_v}|D|_{L^\infty(\overline{\Omega})}\frac{\epsilon_0}{2}\|D^{1/2}\boldsymbol{J}_h^{N+1}\|_0^2+\frac{\tau}{2C_v}|D|_{L^\infty(\overline{\Omega})}\frac{\mu_0}{2}\|D^{1/2}\boldsymbol{K}_h^{N+\frac{3}{2}}\|_0^2\\
&+\left[\frac{1}{C_v}+\tau|\frac{C_m}{2C_v}+\frac{GC_v}{2}|_{L^\infty(\overline{\Omega})}+\frac{\tau}{2C_v}\right]\left(\frac{\mu_0}{2}\|\epsilon_0\boldsymbol{E}_h^{*N+1}\|_0^2+\frac{\epsilon_0}{2}\|\mu_0\boldsymbol{H}_h^{*N+\frac{3}{2}}\|_0^2\right)\\
&+\tau C\sum_{n=0}^{N}\left[\frac{\epsilon_0}{2}\left(\|\boldsymbol{E}_h^n\|_0^2+\|D^{1/2}\boldsymbol{J}_h^n\|_0^2+\|\mu_0\boldsymbol{H}_h^{*n+\frac{1}{2}}\|_0^2\right)\right.\\
&\left.+\frac{\mu_0}{2}\left(\|\boldsymbol{H}_h^{n+\frac{1}{2}}\|_0^2+\|D^{1/2}\boldsymbol{K}_h^{n+\frac{1}{2}}\|_0^2+\|\epsilon_0\boldsymbol{E}_h^{*n}\|_0^2\right)\right],
\end{aligned}
\tag{80}
$$

where the constant C absorbs the explicit dependence on other physical parameters.

Note that $C_v = 3\times 10^8 \gg 1$, which guarantees that the coefficients $\frac{1}{C_v}, \frac{\tau}{2C_v} \ll 1$. Hence, we can choose τ small enough so that the left hand side term of (80) can control the corresponding terms on the right hand side. A specific choice can be

$$\frac{\tau C_v C_{inv}}{h} \leq \frac{1}{2}, \qquad \tau | \frac{C_m}{C_v} + G C_v |_{L^\infty(\overline{\Omega})} \leq \frac{1}{2},$$

which leads to a choice of τ as (51). Applying the discrete Gronwall inequality to (80) completes the proof. □

3.2 The error estimate

For clarity, we use the script letters to descript the corresponding errors. For example, we define the errors between the exact solutions of (12)–(17) and its finite element solutions of (45)–(50):

$$\begin{aligned}
\mathcal{E}^{*n} &:= \boldsymbol{E}^*(t_n) - \boldsymbol{E}_h^{*n} = (\boldsymbol{E}^*(t_n) - \Pi_c \boldsymbol{E}^*(t_n)) \\
&\quad + (\Pi_c \boldsymbol{E}^*(t_n) - \boldsymbol{E}_h^{*n}) := (\boldsymbol{E}^{*n} - \Pi_c \boldsymbol{E}^{*n}) + \mathcal{E}_h^{*n}, \\
\mathcal{H}^{*n+\frac{1}{2}} &:= \boldsymbol{H}^*(t_{n+\frac{1}{2}}) - \boldsymbol{H}_h^{*n+\frac{1}{2}} = (\boldsymbol{H}^*(t_{n+\frac{1}{2}}) - \Pi_d \boldsymbol{H}^*(t_{n+\frac{1}{2}})) \\
&\quad + (\Pi_d \boldsymbol{H}^*(t_{n+\frac{1}{2}}) - \boldsymbol{H}_h^{*n+\frac{1}{2}}) \\
&:= (\boldsymbol{H}^{*n+\frac{1}{2}} - \Pi_d \boldsymbol{H}^{*n+\frac{1}{2}}) + \mathcal{H}_h^{*n+\frac{1}{2}},
\end{aligned}$$

where we denote $\Pi_c \boldsymbol{E}$ and $\Pi_d \boldsymbol{H}$ for the $H(curl;\Omega)$ and $H(div;\Omega)$ interpolations of $\boldsymbol{E}$ and $\boldsymbol{H}$, respectively. Also for simplicity, we denoted $\boldsymbol{E}^{*n} := \boldsymbol{E}^*(t_n)$ and $\boldsymbol{H}^{*n+\frac{1}{2}} := \boldsymbol{H}^*(t_{n+\frac{1}{2}})$. Other errors $\mathcal{J}^{*n}$, $\mathcal{K}^{*n+\frac{1}{2}}$ $\mathcal{E}^n$, $\mathcal{H}^{n+\frac{1}{2}}$ can be definited similarly.

Integrating (14) from t_n to t_{n+1}, multiplying the result by $\frac{1}{\tau}\boldsymbol{\Psi}_h$ and integrating over Ω, then subtracting (45), we obtain

$$\left(\epsilon_0 \frac{\mathcal{E}^{*n+1} - \mathcal{E}^{*n}}{\tau}, \boldsymbol{\Psi}_h \right) = \left(\frac{1}{\tau} \int_{t_n}^{t_{n+1}} \boldsymbol{H} ds - \boldsymbol{H}_h^{n+\frac{1}{2}}, \nabla \times \boldsymbol{\Psi}_h \right),$$

which leads to the error equation

$$\begin{aligned}
&\left(\epsilon_0 \frac{\mathcal{E}_h^{*n+1} - \mathcal{E}_h^{*n}}{\tau}, \boldsymbol{\Psi}_h \right) - \left(\mathcal{H}_h^{n+\frac{1}{2}}, \nabla \times \boldsymbol{\Psi}_h \right) \\
&= \left(\frac{\epsilon_0}{\tau} \int_{t_n}^{t_{n+1}} \partial_t (\Pi_c \boldsymbol{E}^* - \boldsymbol{E}^*) ds, \boldsymbol{\Psi}_h \right) \\
&\quad + \left(\frac{1}{\tau} \int_{t_n}^{t_{n+1}} (\boldsymbol{H} - \Pi_d \boldsymbol{H}^{n+\frac{1}{2}}) ds, \nabla \times \boldsymbol{\Psi}_h \right), \qquad \forall \boldsymbol{\Psi}_h \in \boldsymbol{U}_h^0. \qquad (81)
\end{aligned}$$

Similarly, integrating (15) from $t_{n+\frac{1}{2}}$ to $t_{n+\frac{3}{2}}$, multiplying the result by $\frac{1}{\tau}\boldsymbol{\Phi}_h$ and integrating over Ω, then subtracting (46), we obtain

$$\left(\mu_0 \frac{\mathcal{H}^{*n+\frac{3}{2}} - \mathcal{H}^{*n+\frac{1}{2}}}{\tau}, \boldsymbol{\Phi}_h\right) = -\left(\frac{1}{\tau}\int_{t_{n+\frac{1}{2}}}^{t_{n+\frac{3}{2}}} \nabla \times \boldsymbol{E} ds - \nabla \times \boldsymbol{E}_h^{n+1}, \boldsymbol{\Phi}_h\right),$$

which leads to the error equation

$$\begin{aligned}
&\left(\mu_0 \frac{\mathcal{H}_h^{*n+\frac{3}{2}} - \mathcal{H}_h^{*n+\frac{1}{2}}}{\tau}, \boldsymbol{\Phi}_h\right) + \left(\nabla \times \mathcal{E}_h^{n+1}, \boldsymbol{\Phi}_h\right) \\
&= \left(\frac{\mu_0}{\tau}\int_{t_{n+\frac{1}{2}}}^{t_{n+\frac{3}{2}}} \partial_t(\Pi_d \boldsymbol{H}^* - \boldsymbol{H}^*) ds, \boldsymbol{\Phi}_h\right) \\
&\quad - \left(\frac{1}{\tau}\int_{t_{n+\frac{1}{2}}}^{t_{n+\frac{3}{2}}} \nabla \times (\boldsymbol{E} - \Pi_c \boldsymbol{E}^{n+1}) ds, \boldsymbol{\Phi}_h\right). \qquad \forall \boldsymbol{\Phi}_h \in \boldsymbol{V}_h.
\end{aligned} \tag{82}$$

Integrating (12) from t_n to t_{n+1}, multiplying the result by $\frac{1}{\tau}\widetilde{\boldsymbol{\Psi}}_h$ and integrating over Ω, then subtracting (47), we obtain

$$\left(D\frac{\mathcal{J}^{n+1} - \mathcal{J}^n}{\tau}, \widetilde{\boldsymbol{\Psi}}_h\right) = \left(D(\frac{1}{\tau}\int_{t_n}^{t_{n+1}} \boldsymbol{E} ds - \frac{\boldsymbol{E}_h^{n+1} + \boldsymbol{E}_h^n}{2}), \widetilde{\boldsymbol{\Psi}}_h\right),$$

from which we obtain the third error equation

$$\begin{aligned}
&\left(D\frac{\mathcal{J}_h^{n+1} - \mathcal{J}_h^n}{\tau}, \widetilde{\boldsymbol{\Psi}}_h\right) - \left(D\frac{\mathcal{E}_h^{n+1} + \mathcal{E}_h^n}{2}, \widetilde{\boldsymbol{\Psi}}_h\right) \\
&= \left(\frac{D}{\tau}\int_{t_n}^{t_{n+1}} \partial_t(\Pi_c \boldsymbol{J} - \boldsymbol{J}) ds, \widetilde{\boldsymbol{\Psi}}_h\right) \\
&\quad + \left(\frac{D}{\tau}\int_{t_n}^{t_{n+1}} (\boldsymbol{E} - \Pi_c(\frac{\boldsymbol{E}^{n+1} + \boldsymbol{E}^n}{2})) ds, \widetilde{\boldsymbol{\Psi}}_h\right), \qquad \forall \widetilde{\boldsymbol{\Psi}}_h \in \boldsymbol{U}_h^0.
\end{aligned} \tag{83}$$

Following exactly the same way as deriving (83), we have the fourth error equation

$$\begin{aligned}
&\left(D\frac{\mathcal{K}_h^{n+\frac{3}{2}} - \mathcal{K}_h^{n+\frac{1}{2}}}{\tau}, \widetilde{\boldsymbol{\Phi}}_h\right) - \left(D\frac{\mathcal{H}_h^{n+\frac{3}{2}} + \mathcal{H}_h^{n+\frac{1}{2}}}{2}, \widetilde{\boldsymbol{\Phi}}_h\right) \\
&= \left(\frac{D}{\tau}\int_{t_{n+\frac{1}{2}}}^{t_{n+\frac{3}{2}}} \partial_t(\Pi_d \boldsymbol{K} - \boldsymbol{K}) ds, \widetilde{\boldsymbol{\Phi}}_h\right) \\
&\quad + \left(\frac{D}{\tau}\int_{t_{n+\frac{1}{2}}}^{t_{n+\frac{3}{2}}} (\boldsymbol{H} - \Pi_d(\frac{\boldsymbol{H}^{n+\frac{1}{2}} + \boldsymbol{H}^{n+\frac{3}{2}}}{2})) ds, \widetilde{\boldsymbol{\Phi}}_h\right), \qquad \forall \widetilde{\boldsymbol{\Phi}}_h \in \boldsymbol{V}_h.
\end{aligned} \tag{84}$$

Similarly, integrating (16) from t_n to t_{n+1}, multiplying the result by $\frac{1}{\tau}\widehat{\boldsymbol{\Psi}}_h$ and integrating over Ω, then subtracting (49), we obtain

$$\begin{aligned}
&\left(\frac{\mathcal{E}^{n+1}-\mathcal{E}^{n}}{\tau}, \widehat{\boldsymbol{\Psi}}_h\right) + \left(\frac{C_m}{\tau}\int_{t_n}^{t_{n+1}} (\boldsymbol{E} - \frac{\boldsymbol{E}_h^{n+1}+\boldsymbol{E}_h^{n}}{2})ds, \widehat{\boldsymbol{\Psi}}_h\right)\\
&\quad + \left(\frac{D}{\tau}\int_{t_n}^{t_{n+1}} (\boldsymbol{J} - \frac{\boldsymbol{J}_h^{n+1}+\boldsymbol{J}_h^{n}}{2})ds, \widehat{\boldsymbol{\Psi}}_h\right)\\
&\quad = \left(\frac{\mathcal{E}^{*n+1}-\mathcal{E}^{*n}}{\tau}, \widehat{\boldsymbol{\Psi}}_h\right) + \left(\frac{G}{\tau}\int_{t_n}^{t_{n+1}} (\boldsymbol{E}^* - \frac{\boldsymbol{E}_h^{*n+1}+\boldsymbol{E}_h^{*n}}{2})ds, \widehat{\boldsymbol{\Psi}}_h\right),
\end{aligned}$$

which leads to the fifth error equation

$$\begin{aligned}
&\left(\frac{\mathcal{E}_h^{n+1}-\mathcal{E}_h^{n}}{\tau}, \widehat{\boldsymbol{\Psi}}_h\right) + \left(C_m\frac{\mathcal{E}_h^{n+1}+\mathcal{E}_h^{n}}{2}, \widehat{\boldsymbol{\Psi}}_h\right) + \left(D\frac{\mathcal{J}_h^{n+1}+\mathcal{J}_h^{n}}{2}, \widehat{\boldsymbol{\Psi}}_h\right)\\
&\quad - \left(\frac{\mathcal{E}_h^{*n+1}-\mathcal{E}_h^{*n}}{\tau}, \widehat{\boldsymbol{\Psi}}_h\right) - \left(G\frac{\mathcal{E}_h^{*n+1}+\mathcal{E}_h^{*n}}{2}, \widehat{\boldsymbol{\Psi}}_h\right)\\
&\quad = \left(\frac{1}{\tau}\int_{t_n}^{t_{n+1}} \partial_t(\Pi_c\boldsymbol{E} - \boldsymbol{E})ds, \widehat{\boldsymbol{\Psi}}_h\right)\\
&\qquad + \left(\frac{C_m}{\tau}\int_{t_n}^{t_{n+1}} (\Pi_c(\frac{\boldsymbol{E}^{n+1}+\boldsymbol{E}^{n}}{2}) - \boldsymbol{E})ds, \widehat{\boldsymbol{\Psi}}_h\right)\\
&\qquad + \left(\frac{D}{\tau}\int_{t_n}^{t_{n+1}} (\Pi_c(\frac{\boldsymbol{J}^{n+1}+\boldsymbol{J}^{n}}{2}) - \boldsymbol{J})ds, \widehat{\boldsymbol{\Psi}}_h\right)\\
&\qquad + \left(\frac{1}{\tau}\int_{t_n}^{t_{n+1}} \partial_t(\boldsymbol{E}^* - \Pi_c\boldsymbol{E}^*)ds, \widehat{\boldsymbol{\Psi}}_h\right)\\
&\qquad + \left(\frac{G}{\tau}\int_{t_n}^{t_{n+1}} (\boldsymbol{E}^* - \Pi_c(\frac{\boldsymbol{E}^{*n+1}+\boldsymbol{E}^{*n}}{2}))ds, \widehat{\boldsymbol{\Psi}}_h\right), \qquad \forall \widehat{\boldsymbol{\Psi}}_h \in \boldsymbol{U}_h^0.
\end{aligned} \tag{85}$$

Following exactly the same way as deriving (85), we have the sixth error equation: For any $\widehat{\boldsymbol{\Phi}}_h \in \boldsymbol{V}_h$,

$$\begin{aligned}
&\left(\frac{\mathcal{H}_h^{n+\frac{3}{2}}-\mathcal{H}_h^{n+\frac{1}{2}}}{\tau}, \widehat{\boldsymbol{\Phi}}_h\right) + \left(C_m\frac{\mathcal{H}_h^{n+\frac{3}{2}}+\mathcal{H}_h^{n+\frac{1}{2}}}{2}, \widehat{\boldsymbol{\Phi}}_h\right) + \left(D\frac{\mathcal{K}_h^{n+\frac{3}{2}}+\mathcal{K}_h^{n+\frac{1}{2}}}{2}, \widehat{\boldsymbol{\Phi}}_h\right)\\
&\quad - \left(\frac{\mathcal{H}_h^{*n+\frac{3}{2}}-\mathcal{H}_h^{*n+\frac{1}{2}}}{\tau}, \widehat{\boldsymbol{\Phi}}_h\right) - \left(G\frac{\mathcal{H}_h^{*n+\frac{3}{2}}+\mathcal{H}_h^{*n+\frac{1}{2}}}{2}, \widehat{\boldsymbol{\Phi}}_h\right)\\
&\quad = \left(\frac{1}{\tau}\int_{t_{n+\frac{1}{2}}}^{t_{n+\frac{3}{2}}} \partial_t(\Pi_d\boldsymbol{H} - \boldsymbol{H})ds, \widehat{\boldsymbol{\Phi}}_h\right)
\end{aligned}$$

$$+\left(\frac{C_m}{\tau}\int_{t_{n+\frac{1}{2}}}^{t_{n+\frac{3}{2}}}(\Pi_d(\frac{\boldsymbol{H}^{n+\frac{3}{2}}+\boldsymbol{H}^{n+\frac{1}{2}}}{2})-\boldsymbol{H})ds,\widehat{\boldsymbol{\Phi}}_h\right)$$
$$+\left(\frac{D}{\tau}\int_{t_{n+\frac{1}{2}}}^{t_{n+\frac{3}{2}}}(\Pi_d(\frac{\boldsymbol{K}^{n+\frac{3}{2}}+\boldsymbol{K}^{n+\frac{1}{2}}}{2})-\boldsymbol{K})ds,\widehat{\boldsymbol{\Phi}}_h\right)$$
$$+\left(\frac{1}{\tau}\int_{t_{n+\frac{1}{2}}}^{t_{n+\frac{3}{2}}}\partial_t(\boldsymbol{H}^*-\Pi_d\boldsymbol{H}^*)ds,\widehat{\boldsymbol{\Phi}}_h\right)$$
$$+\left(\frac{G}{\tau}\int_{t_{n+\frac{1}{2}}}^{t_{n+\frac{3}{2}}}(\boldsymbol{H}^*-\Pi_d(\frac{\boldsymbol{H}^{*n+\frac{3}{2}}+\boldsymbol{H}^{*n+\frac{1}{2}}}{2}))ds,\widehat{\boldsymbol{\Phi}}_h\right). \tag{86}$$

Note that the error equations (81)–(86) have exactly the same form as the finite element scheme (45)–(50), except those extra terms added to the right hand sides of (81)–(86) due to the time and spatial discretization. Moreover, by the interpolation error extimates of Π_c and Π_d, these extra terms have the local truncation errors $O(\tau^2+h^l)$, where $l\geq 1$ is the degree of the basis function in the finite element spaces $\boldsymbol{V}_h$ and $\boldsymbol{U}_h$. Hence, by following the same technique developed for proving the discrete stability given in Theorem 2, we can prove the following error estimate between the interpolation and the finite element solution:

$$\begin{aligned}
&\frac{\epsilon_0}{2}\left(\|\mathcal{E}_h^{N+1}\|_0^2+\|D^{1/2}\mathcal{J}_h^{N+1}\|_0^2+\|\mu_0\mathcal{H}_h^{*N+\frac{3}{2}}\|_0^2\right)\\
&\quad+\frac{\mu_0}{2}\left(\|\mathcal{H}_h^{N+\frac{3}{2}}\|_0^2+\|D^{1/2}\mathcal{K}_h^{N+\frac{3}{2}}\|_0^2+\|\epsilon_0\mathcal{E}_h^{*N+1}\|_0^2\right)\\
&\leq C\left[\frac{\epsilon_0}{2}\left(\|\mathcal{E}_h^0\|_0^2+\|D^{1/2}\mathcal{J}_h^0\|_0^2+\|\mu_0\mathcal{H}_h^{*\frac{1}{2}}\|_0^2\right)\right.\\
&\quad\left.+\frac{\mu_0}{2}\left(\|\mathcal{H}_h^{\frac{1}{2}}\|_0^2+\|D^{1/2}\mathcal{K}_h^{\frac{1}{2}}\|_0^2+\|\epsilon_0\mathcal{E}_h^{*0}\|_0^2\right)+(\tau^2+h^l)^2\right].
\end{aligned}\tag{87}$$

By choosing the following initial conditions

$$\boldsymbol{E}_h^0=\Pi_c\boldsymbol{E}(0),\ \boldsymbol{E}_h^{*0}=\Pi_c\boldsymbol{E}^*(0),\ \boldsymbol{J}_h^0=\Pi_c\boldsymbol{J}(0),$$
$$\boldsymbol{H}_h^0=\Pi_d\boldsymbol{H}(0),\ \boldsymbol{H}_h^{*0}=\Pi_d\boldsymbol{H}^*(0),\ \boldsymbol{K}_h^0=\Pi_d\boldsymbol{K}(0),$$

then using the triangle inequality and the interpolation error extimates of Π_c and Π_d to (87), we can obtain the following optimal error estimate between the analytical solution and the finite element solution:

$$\begin{aligned}
&\frac{\epsilon_0}{2}\left(\|\mathcal{E}^{N+1}\|_0^2+\|D^{1/2}\mathcal{J}^{N+1}\|_0^2+\|\mu_0\mathcal{H}^{*N+\frac{3}{2}}\|_0^2\right)\\
&\quad+\frac{\mu_0}{2}\left(\|\mathcal{H}^{N+\frac{3}{2}}\|_0^2+\|D^{1/2}\mathcal{K}^{N+\frac{3}{2}}\|_0^2+\|\epsilon_0\mathcal{E}^{*N+1}\|_0^2\right)
\end{aligned}$$

$$\leq C(\tau^2 + h^l)^2. \tag{88}$$

4 Numerical results

In this section, we present some numerical results to demonstrate the performance of this Cohen–Monk PML model. For simplicity, we focus on solving the 2D version of the numerical scheme (45)–(50). More specifically, we consider the so-called TE_z mode, which has unknowns $\boldsymbol{E} = [E_x, E_y]^T, H_z, \boldsymbol{E}^* = [E_x^*, E_y^*]^T, H_z^*, \boldsymbol{J} = [J_x, J_y]^T$, K_z, and the governing equations are given as follow:

$$\frac{\partial \boldsymbol{J}}{\partial t} = \boldsymbol{E}, \tag{89}$$
$$\frac{\partial K_z}{\partial t} = H_z, \tag{90}$$
$$\epsilon_0 \frac{\partial \boldsymbol{E}^*}{\partial t} - \nabla \times H_z = 0, \tag{91}$$
$$\mu_0 \frac{\partial H_z^*}{\partial t} + \nabla \times \boldsymbol{E} = 0, \tag{92}$$
$$\frac{\partial \boldsymbol{E}}{\partial t} + C_{2d}\boldsymbol{E} + D_{2d}\boldsymbol{J} = \frac{\partial \boldsymbol{E}^*}{\partial t} + G_{2d}\boldsymbol{E}^* + \boldsymbol{f}, \tag{93}$$
$$\frac{\partial H_z}{\partial t} + C_{1d}H_z + D_{1d}K_z = \frac{\partial H_z^*}{\partial t} + G_{1d}H_z^* + g_z, \tag{94}$$

where the curls $\nabla \times \boldsymbol{E} = \frac{\partial E_y}{\partial x} - \frac{\partial E_x}{\partial y}$, $\nabla \times H_z = [\frac{\partial H_z}{\partial y}, -\frac{\partial H_z}{\partial x}]^T$, and the definitions of $\boldsymbol{f} = [f_x, f_y]^T$, $\boldsymbol{g} = g_z$ can be derived similarly from the 3D model. Moreover,

$$C_{2d} = diag(\sigma_2, \sigma_1), \quad D_{2d} = diag(0, 0), \quad G_{2d} = diag(\sigma_1, \sigma_2),$$
$$C_{1d} = \sigma_1 + \sigma_2, \quad D_{1d} = \sigma_1\sigma_2, \quad G_{1d} = 0.$$

Since $D_{2d} = diag(0, 0)$, the function $\boldsymbol{J}$ is not used in (93). Hence the equation (89) is not needed in the 2D model. For simplicity, we only employ the lowest order Raviart-Thomas-Nédélec mixed spaces on rectangular elements [14]:

$$\mathbf{V}_h = \left\{\psi_h \in L^2(\Omega) : \psi_h\big|_K = Q_{0,0}, \forall K \in T_h\right\},$$
$$\mathbf{U}_h = \left\{\phi_h \in H(curl; \Omega) : \phi_h\big|_K = Q_{0,1} \times Q_{1,0}, \forall K \in T_h\right\},$$

where $Q_{i,j}$ denotes the set of polynomials of degrees of i and j in the x and y directions, respectively.

Example 1 This example is used to justify the convergence rate of our scheme. To construct an analytical solution, we add extra source terms $\hat{\boldsymbol{f}} = [\bar{f}_x, \hat{f}_y]^T$, $\hat{g}_z$ and g_z^* to the model equations (89)–(94), and choose the physical domain $\Omega = [0, 1]^2$ and

$$\epsilon_0 = \mu_0 = 1, \qquad \sigma_1(x) = \sin^2(\pi x), \qquad \sigma_2(y) = \sin^2(\pi y).$$

More specifically, we solve the following governing equations:

$$\frac{\partial K_z}{\partial t} = H_z, \tag{95}$$

$$\epsilon_0 \frac{\partial \boldsymbol{E}^*}{\partial t} - \nabla \times H_z = 0, \tag{96}$$

$$\mu_0 \frac{\partial H_z^*}{\partial t} + \nabla \times \boldsymbol{E} = g_z^*, \tag{97}$$

$$\frac{\partial \boldsymbol{E}}{\partial t} + C_{2d}\boldsymbol{E} = \frac{\partial \boldsymbol{E}^*}{\partial t} + G_{2d}\boldsymbol{E}^* + \boldsymbol{f} + \hat{\boldsymbol{f}}, \tag{98}$$

$$\frac{\partial H_z}{\partial t} + C_{1d}H_z + D_{1d}K_z = \frac{\partial H_z^*}{\partial t} + G_{1d}H_z^* + g_z + \hat{g}_z, \tag{99}$$

such that the exact solution is given as follows:

$$\begin{aligned} &\boldsymbol{E} = \begin{pmatrix} E_x \\ E_y \end{pmatrix} = \begin{pmatrix} e^{-\pi t}\cos(\pi x)\sin(\pi y) \\ -e^{-\pi t}\sin(\pi x)\cos(\pi y) \end{pmatrix}, \ \boldsymbol{E}^* = \boldsymbol{E}, \\ &H_z = e^{-\pi t}\cos(\pi x)\cos(\pi y), \ K_z = -\frac{1}{\pi}e^{-\pi t}\cos(\pi x)\cos(\pi y), \ H_z^* = H_z. \end{aligned} \tag{100}$$

The corresponding source terms are given as:

$$\begin{aligned} &\boldsymbol{f} = \begin{pmatrix} f_x \\ f_y \end{pmatrix} = \begin{pmatrix} \cos(\pi x)\sin(\pi y)\left(\sin^2(\pi y) - \sin^2(\pi x)\right) \\ \sin(\pi x)\cos(\pi y)\left(\sin^2(\pi y) - \sin^2(\pi x)\right) \end{pmatrix}, \\ &\hat{\boldsymbol{f}} = \begin{pmatrix} \hat{f}_x \\ \hat{f}_y \end{pmatrix} = \begin{pmatrix} e^{-\pi t}\cos(\pi x)\sin(\pi y)\left(\sin^2(\pi y) - \sin^2(\pi x)\right) \\ e^{-\pi t}\sin(\pi x)\cos(\pi y)\left(\sin^2(\pi y) - \sin^2(\pi x)\right) \end{pmatrix} - \boldsymbol{f}, \\ &g_z = \cos(\pi x)\cos(\pi y)\left(\sin^2(\pi x) + \sin^2(\pi y)\right), \\ &\hat{g}_z = e^{-\pi t}\cos(\pi x)\cos(\pi y)\left[\left(\sin^2(\pi x) + \sin^2(\pi y)\right) - \frac{1}{\pi}\sin^2(\pi x)\sin^2(\pi y)\right] - g_z, \\ &g_z^* = -3\pi e^{-\pi t}\cos(\pi x)\cos(\pi y). \end{aligned} \tag{101}$$

Modification of the 3D numerical scheme (45)–(50) to solve (95)–(99) leads to the following 2D scheme: find $\boldsymbol{E}_h^{n+1}, \boldsymbol{E}_h^{*n+1} \in \mathbf{U}_h^0, H_h^{n+\frac{3}{2}}, H_h^{*n+\frac{3}{2}}, K_h^{n+\frac{3}{2}} \in \mathbf{V}_h$ such that

$$\left(\sigma_1\sigma_2 \frac{K_h^{n+\frac{3}{2}} - K_h^{n+\frac{1}{2}}}{\tau}, \widetilde{\Phi}_h\right) = \left(\sigma_1\sigma_2 \frac{H_h^{n+\frac{3}{2}} + H_h^{n+\frac{1}{2}}}{2}, \widetilde{\Phi}_h\right), \qquad \forall \widetilde{\Phi}_h \in \boldsymbol{V}_h, \tag{102}$$

$$\left(\epsilon_0 \frac{\boldsymbol{E}_h^{*n+1} - \boldsymbol{E}_h^{*n}}{\tau}, \boldsymbol{\Psi}_h\right) = \left(H_h^{n+\frac{1}{2}}, \nabla \times \boldsymbol{\Psi}_h\right), \qquad \forall \boldsymbol{\Psi}_h \in \boldsymbol{U}_h^0, \tag{103}$$

$$\left(\mu_0 \frac{H_h^{*n+\frac{3}{2}} - H_h^{*n+\frac{1}{2}}}{\tau}, \Phi_h\right) = -\left(\nabla \times \boldsymbol{E}_h^{n+1}, \Phi_h\right) + \left(g_z^*(t_{n+1}), \Phi_h\right), \qquad \forall \Phi_h \in \boldsymbol{V}_h, \tag{104}$$

$$\left(\frac{\boldsymbol{E}_h^{n+1} - \boldsymbol{E}_h^n}{\tau}, \widehat{\boldsymbol{\Psi}}_h\right) + \left(C_{2d}\frac{\boldsymbol{E}_h^{n+1} + \boldsymbol{E}_h^n}{2}, \widehat{\boldsymbol{\Psi}}_h\right)$$

Table 1 The L_∞ and L_2 errors obtained with $\tau = 10^{-5}$ at 1000 time steps

h	$\lvert \boldsymbol{E} - \boldsymbol{E}_h \rvert$		Rate		$\lvert H - H_h \rvert$		Rate	
	L_∞	L_2	L_∞	L_2	L_∞	L_2	L_∞	L_2
$\frac{1}{10}$	1.6094×10^{-2}	5.8090×10^{-3}	–	–	7.2153×10^{-4}	2.2760×10^{-4}	–	–
$\frac{1}{20}$	4.0924×10^{-3}	1.4494×10^{-3}	1.9755	2.0028	1.8669×10^{-4}	5.7065×10^{-5}	1.9504	1.9958
$\frac{1}{40}$	1.0275×10^{-3}	3.6217×10^{-4}	1.9939	2.0007	4.7076×10^{-5}	1.4276×10^{-5}	1.9876	1.9990
$\frac{1}{80}$	2.5714×10^{-4}	9.0532×10^{-5}	1.9985	2.0002	1.1795×10^{-5}	3.5697×10^{-6}	1.9969	1.9997
$\frac{1}{160}$	6.4301×10^{-5}	2.2632×10^{-5}	1.9996	2.0000	2.9502×10^{-6}	8.9247×10^{-7}	1.9992	1.9999

Table 2 The L_∞ and L_2 errors obtained with $\tau = h/4$ at $T = 1$

h	$\|\boldsymbol{E} - \boldsymbol{E}_h\|$		Rate		$\|H - H_h\|$		Rate	
	L_∞	L_2	L_∞	L_2	L_∞	L_2	L_∞	L_2
$\frac{1}{10}$	7.6123×10^{-3}	2.4075×10^{-3}	–	–	6.5191×10^{-3}	2.2776×10^{-3}	–	–
$\frac{1}{20}$	1.9763×10^{-3}	5.9210×10^{-4}	1.9455	2.0236	1.7582×10^{-3}	6.1294×10^{-4}	1.8906	1.8937
$\frac{1}{40}$	4.9880×10^{-4}	1.4707×10^{-4}	1.9863	2.0094	4.5159×10^{-4}	1.5804×10^{-4}	1.9610	1.9555
$\frac{1}{80}$	1.2497×10^{-4}	3.6663×10^{-5}	1.9969	2.0041	1.1425×10^{-4}	4.0069×10^{-5}	1.9828	1.9797
$\frac{1}{160}$	3.1256×10^{-5}	9.1538×10^{-6}	1.9994	2.0019	2.8725×10^{-5}	1.0085×10^{-5}	1.9918	1.9903

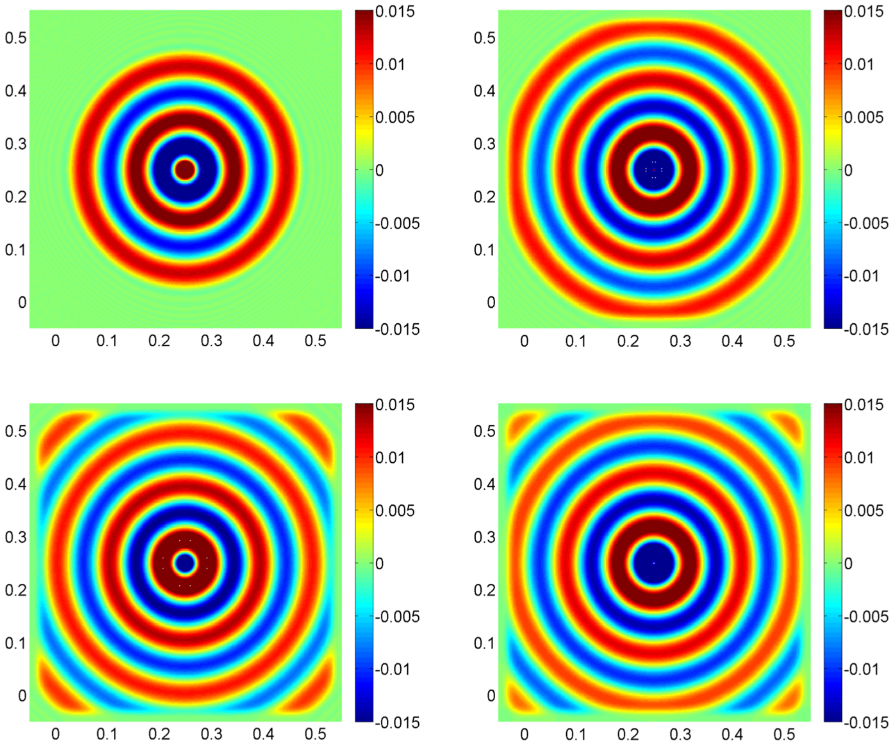

Fig. 1 Snapshots of the magnetic field H_z: (top left) 300 steps; (top right) 400 steps; (bottom left) 500 steps; and (bottom right) 10,000 steps

$$= \left(\frac{\boldsymbol{E}_h^{*n+1} - \boldsymbol{E}_h^{*n}}{\tau}, \widehat{\boldsymbol{\Psi}}_h \right) + \left(G_{2d} \frac{\boldsymbol{E}_h^{*n+1} + \boldsymbol{E}_h^{*n}}{2}, \widehat{\boldsymbol{\Psi}}_h \right) + \left((\boldsymbol{f} + \hat{\boldsymbol{f}})(t_{n+\frac{1}{2}}), \widehat{\boldsymbol{\Psi}}_h \right), \qquad \forall \widehat{\boldsymbol{\Psi}}_h \in \boldsymbol{U}_h^0, \tag{105}$$

$$\left(\frac{H_h^{n+\frac{3}{2}} - H_h^{n+\frac{1}{2}}}{\tau}, \widehat{\Phi}_h \right) + \left((\sigma_1 + \sigma_2) \frac{H_h^{n+\frac{3}{2}} + H_h^{n+\frac{1}{2}}}{2}, \widehat{\Phi}_h \right)$$
$$+ \left(\sigma_1 \sigma_2 \frac{K_h^{n+\frac{3}{2}} + K_h^{n+\frac{1}{2}}}{2}, \widehat{\Phi}_h \right) = \left(\frac{H_h^{*n+\frac{3}{2}} - H_h^{*n+\frac{1}{2}}}{\tau}, \widehat{\Phi}_h \right)$$
$$+ \left((g_z + \hat{g}_z)(t_{n+1}), \widehat{\Phi}_h \right), \qquad \forall \widehat{\Phi}_h \in \boldsymbol{V}_h. \tag{106}$$

We solve this model problem with a time step size $\tau = 10^{-5}$ and varying mesh sizes h from $\frac{1}{10}$ to $\frac{1}{160}$ and runs for 1000 time steps. The convergence rates are presented in Table 1, which clearly shows $\mathcal{O}(h^2)$ in both L_∞ and the discrete L_2 norms (the numerical quadrature calculated at element centers). Note that $\mathcal{O}(h^2)$ in both L_∞ and the discrete L_2 norms is a superconvergence result, which has been proved and observed for the lowest-order rectangular and cubic edge element [10,12].

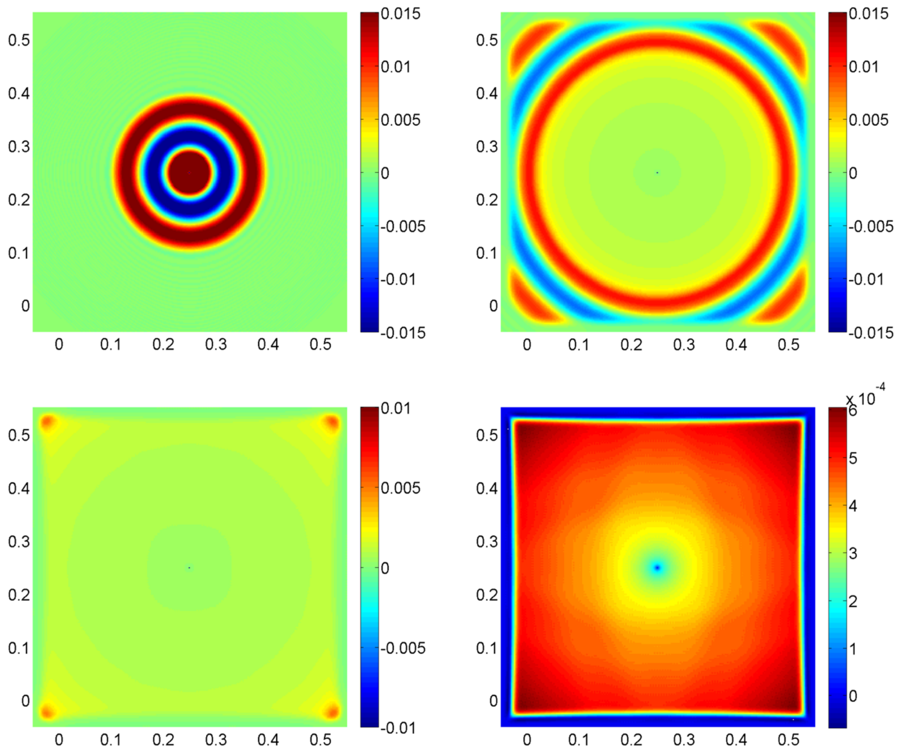

Fig. 2 Magnetic field H_z at various time steps: (top left) 200 steps; (top right) 500 steps; (bottom left) 700 steps; and (bottom right) 1000 steps

In Table 2, we present the numerical results obtained with varying mesh sizes h from $\frac{1}{10}$ to $\frac{1}{160}$, time step size $\tau = h/4$, and the final simulation time $T = 1$. Table 2 shows $\mathcal{O}(\tau^2)$ in both L_∞ and discrete L_2 norms.

Example 2 In this example, we choose the same benchmark problem developed in our previous paper [9] to compare how the current algorithm works. More specifically, we choose the physical domain $\Omega = [0, 0.5]m \times [0, 0.5]m$, which is divided by uniform rectangles with mesh size $h = 2.5 \times 10^{-3}m$ and time step size $\tau = 2.5 \times 10^{-12}s$. We surround the physical domain by a PML with thickness $dd = 20h$. In our simulation, the damping function σ_1 is chosen as a fourth-order polynomial function given as:

$$\sigma_1(x) = \begin{cases} \sigma_{max}(\frac{x-0.5}{dd})^4, & \text{if } x \geq 0.5, \\ \sigma_{max}(\frac{x}{dd})^4, & \text{if } x \leq 0.0, \\ 0, & \text{elsewhere,} \end{cases}$$

where $\sigma_{max} = -log(err) * 5 * 0.07 * C_v/(2 * dd)$ with $err = 10^{-7}$. Recall that C_v denotes the wave propagation speed in vacuum. The damping function σ_2 has exactly the same form but varies in y variable.

In this example, we solve the scheme (102)–(106) with no added source terms $\hat{\boldsymbol{f}}$, $\hat{g}_z$, g_z^*, and zero initial fields (which means that $\boldsymbol{f} = \mathbf{0}$, $g_z = 0$). We choose a point incident source wave located at point (0.25, 0.25) and imposed as

$$H_z = 0.1 \sin(2\pi \nu t), \qquad \text{where} \ \ \nu = 3GHz.$$

In Fig. 1, we plot some snapshots of the magnetic field H_z obtained by our scheme. To see the long time stability of our scheme, we plot the field H_z up to 10,000 time steps.

To see how the PML performs, we solve this example again by stopping the source wave after 200 time steps. The computed magnetic fields H_z at various time steps are plotted in Fig. 2, which shows that the source wave exits the domain without obvious reflections. Small remaining wave inside the physical domain is due to the numerical error caused by the mesh size and the low accuracy of the scheme.

5 Conclusion

In this paper, we first reformulated an equivalent Cohen–Monk PML model and then proved its stability. A finite element method is proposed to solve this equivalent PML model, and its numerical stability and optimal error estimate are proved. Numerical results demonstrating the effectiveness of this PML model are presented. In the future, we can consider the 3D implementation of this PML model and its application.

References

1. Appelö, D., Hagstrom, T., Kreiss, G.: Perfectly matched layers for hyperbolic systems: general formulation, well-posedness, and stability. SIAM J. Appl. Math. **67**(1), 1–23 (2006)
2. Bao, G., Li, P., Wu, H.: An adaptive edge element method with perfectly matched absorbing layers for wave scattering by biperiodic structures. Math. Comp. **79**, 1–34 (2010)
3. Bécache, E., Joly, P., Kachanovska, M., Vinoles, V.: Perfectly matched layers in negative index metamaterials and plasmas. ESAIM Proc. Surv. **50**, 113–132 (2015)
4. Bérenger, J.P.: A perfectly matched layer for the absorbing EM waves. J. Comput. Phys. **114**, 185–200 (1994)
5. Bokil, V.A., Buksas, M.W.: Comparison of finite difference and mixed finite element methods for perfectly matched layer models. Commun. Comput. Phys. **2**, 806–826 (2007)
6. Bonnet-Ben Dhia, A.-S., Carvalho, C., Chesnel, L., Ciarlet Jr., P.: On the use of perfectly matched layers at corners for scattering problems with sign-changing coefficients. J. Comput. Phys. **322**, 224–247 (2016)
7. Cohen, G.C., Monk, P.: Mur-Nédélec finite element schemes for Maxwell's equations. Comput. Methods Appl. Mech. Eng. **169**, 197–217 (1999)
8. Hong, J.L., Ji, L.H., Kong, L.H.: Energy-dissipation splitting finite-difference time-domain method for Maxwell equations with perfectly matched layers. J. Comput. Phys. **269**, 201–214 (2014)
9. Huang, Y., Li, J., Yang, W.: Mathematical analysis of a PML model obtained with stretched coordinates and its application to backward wave propagation in metamaterials. Numer. Methods Part. Differ. Eq. **30**, 1558–1574 (2014)
10. Huang, Y., Li, J., Yang, W., Sun, S.: Superconvergence of mixed finite element approximations to 3-D Maxwell's equations in metamaterials. J. Comput. Phys. **230**, 8275–8289 (2011)
11. Kong, L.H., Hong, Y.Q., Tian, N.N., Zhang, P.: Stable and efficient numerical schemes Maxwell equations in lossy medium. J. Comput. Phys. **397**, 108703 (2019)

12. Li, J.: Finite element study of the Lorentz model in metamaterials. Comput. Methods Appl. Mech. Eng. **200**, 626–637 (2011)
13. Li, J., Hesthaven, J.S.: Analysis and application of the nodal discontinuous Galerkin method for wave propagation in metamaterials. J. Comput. Phys. **258**, 915–930 (2014)
14. Li, J., Huang, Y.: Time-Domain Finite Element Methods for Maxwell's Equations in Metamaterials, Springer Series in Computational Mathematics, vol. 43. Springer, Berlin (2013)
15. Lin, Y., Zhang, K., Zou, J.: Studies on some perfectly matched layers for one-dimensional time-dependent systems. Adv. Comput. Math. **30**, 1–35 (2009)
16. Monk, P.: Finite Element Methods for Maxwell's Equations. Oxford University Press, Oxford (2003)
17. Taflove, A., Haguess, S.C.: Computational Electrodynamics: The Finite-Difference Time-Domain Method, 3rd edn. Artech House, Norwood (2005)